NASA Contractor Report 3288

General Design Method for Three-Dimensional, Potential Flow Fields

I - Theory

John D. Stanitz

CONTRACT NAS3-21605
AUGUST 1980

NASA

NASA Contractor Report 3288

General Design Method for Three-Dimensional, Potential Flow Fields

I - Theory

John D. Stanitz
John D. Stanitz, Consulting Engineer
University Heights, Ohio

Prepared for
Lewis Research Center
under Contract NAS3-21605

NASA
National Aeronautics
and Space Administration

Scientific and Technical
Information Branch

1980

CONTENTS

SUMMARY

The general design method developed in this report is for steady, three-dimensional, potential, incompressible or subsonic-compressible flow. In this design method, the flow field, including the shape of its boundary, is determined for arbitrarily specified, continuous distributions of velocity as a function of arc length along the boundary streamlines. The method applies to the design of both internal and external flow fields, including, in both cases, fields with planar symmetry. These designs result from the finite-difference solution of a governing, partial-differential equation for the distribution of velocity in transformed space, the coordinates of which are the velocity potential and two stream functions. The analytic problems associated with stagnation points, closure of bodies in external flow fields, and prediction of turning angles in three-dimensional ducts are discussed, but not treated in detail.

This three-dimensional design method applies to simple ducts, branched ducts, annular ducts, and ducts with centerbodies (including the nose and/or tail region) and to ducted or nonducted bodies in infinite, uniform flow fields.

INTRODUCTION

In the theory of multidimensional, potential flow there are two kinds of boundary-value problems: (1) the direct problem, in which the distribution of velocity is determined for a prescribed shape of the boundary and (2) the inverse problem, in which the shape of the boundary is determined for a prescribed distribution of velocity along it. The direct problem is an analysis problem; the inverse problem is a design problem. This report is concerned with the inverse, or design, problem for steady, three-dimensional, subsonic, potential flow through ducts, or around bodies, with prescribed velocities as a function of arc length in the direction of flow along the boundary of the field.

The design of flow fields with satisfactory velocities along the boundary is important for the following reasons:

(1) Boundary-layer separation losses can be avoided by prescribed velocity distributions in the direction of flow, along the material surfaces of the boundary, that do not decrease too rapidly.

(2) Shock losses in compressible flow, and cavitation in incompressible flow, can be avoided by prescribed velocities that do not exceed certain maximum values dictated by these phenomena.

(3) For compressible flow in ducts, the desired flow rate can be assured by prescribed velocities that do not result in premature choked flow.

However, the first objective of fluid dynamic design is to determine the shape of the boundary of the flow field for which losses are minimum. For both incompressible and shock-free compressible flow, fluid losses originate at the material surfaces along the boundary of the flow field, and the magnitude of these losses depends on the velocity distribution along these surfaces. The characteristics of a desirable velocity distribution are relatively well-known from boundary-layer theory.

Solutions of either the design or analysis type of boundary-value problem can be used to obtain a satisfactory velocity distribution. In the inverse, design method, an acceptable velocity distribution is specified, and the resulting shape of the flow field determined. If for some reason the shape is unsatisfactory, the prescribed velocity distribution can be modified, and the solution repeated until an acceptable shape is achieved. In the direct, analysis method, on the other hand, an acceptable shape is specified, and the resulting velocity distribution determined. If this velocity distribution is unsatisfactory, the shape can be modified until an acceptable distribution is achieved.

With either method, the final design is usually arrived at only after iterating on the specified input. The inverse, design method, however, has some advantage, because it starts with an acceptable velocity distribution and because, in some cases, it arrives at boundary shapes that could not otherwise be envisioned by the designer.

The previous discussion applies both to internal flow fields, in which the boundary surrounds the flow, as in ducts, and to external flow fields, in which the flow surrounds the bounding surface, as on bodies.

The general design method developed in this report is for three-dimensional, potential, incompressible or subsonic-compressible flow. The method applies to the design of both internal and external flow fields, including, in both cases, fields with planar symmetry. For plane, two-dimensional flow, design methods have been developed in the past for internal flow fields (e.g., ref. 1), and numerous methods have also been developed for external flow fields. For axisymmetric, two-dimensional flow, a design method has been developed recently for internal flow fields (ref. 2), but no similar design method appears to have been attempted for external flow. Until now, no general three-dimensional design method has existed for either internal or external flow fields.

A major difficulty faced by all the design methods just mentioned is that they are boundary-value problems in which the velocity distribution is specified along physical boundaries, the shapes of which are not known until the problem is solved. In the two-dimensional cases, this difficulty has been avoided by solving the boundary-value problem in the transformed plane of the velocity potential φ and the stream function ψ. In the present three-dimensional case, the difficulty is avoided by solving the problem in φ, ψ, η-space, where η is a second stream function associated with continuity in three-dimensional flow (ref. 3).

Because of its general nature, the method of this report is not likely to be used for the design of flow fields with special physical characteristics, such as the hub and shroud surfaces of revolution in turbomachines. These particular surfaces, for example, should be more easily designed by using the method developed in reference 2 for axisymmetric flow. However, as is demonstrated later in this report, the design methods for plane, two-dimensional flow (e.g., ref. 1) and for axisymmetric, two-dimensional flow (ref. 2) are special cases of the general, governing differential equation developed in this report.

Finally, the analyses of this first report do not treat problems associated with the following three important boundary conditions: (1) stagnation points, (2) body closure, and (3) duct turning. Thus, in this analysis, any region in the vicinity of what would normally be a stagnation point is cusped; body closure can be assured only when a plane of symmetry exists that is normal to the direction of undisturbed flow (otherwise the body will likely have a tail of essentially constant cross section that trails downstream to infinity); and the desired duct turning can be achieved only by trial-and-error iteration of the specified velocity distribution on the boundary of the flow field.

SYMBOLS

All quantities are nondimensional unless otherwise specified.

A	local continuity parameter, eqs. (10a) and (10g)
A_U	upstream boundary area, 1.0 in nondimensional form
a	distance between adjacent nodal points of finite-difference star, fig. 10
B	local continuity parameter, eqs. (10b) and (10e)
C	constant
$C_C, C_0, C_1, \ldots, C_6$	coefficients in governing finite-difference eq. (28e), eqs. (28f)
$C_1^*, C_2^*, C_3^*, C_4^*$	coefficients given by eqs. (21f), (22f), and (23f)
c	local speed of sound, m/sec, eq. (3b)
E, F, G	coefficients of first fundamental quadratic form of surface geometry, eqs. (A3)
$\bar{e}$	unit tangent vector
$\bar{e}_1$	unit vector in direction of q along streamlines, which are intersections of ψ and η stream surfaces, fig. 3 and eq. (7a)

$\bar{e}_2$	unit vector tangent to intersection of η stream surface and φ potential surface, fig. 3 and eq. (7c)
$\bar{e}_3$	unit vector tangent to intersection of ψ stream surface and φ potential surface, fig. 3 and eq. (7e)
H	$(\partial\bar{r}/\partial u) \times (\partial\bar{r}/\partial v) \cdot \bar{n}$, eq. (B2)
h	enthalpy, J/kg
$\bar{i}, \bar{j}, \bar{k}$	unit vectors in x-, y-, and z-directions, respectively
K_η, K_ψ	total curvatures of η and ψ stream surfaces, respectively, eqs. (17f) and (17g) (also (C5) and (C6))
k	nondimensional parameter, eq. (4e)
M	local Mach number, eq. (3a)
m	path length in direction of $\bar{e}_3$ along intersection of ψ stream surface and φ potential surface, fig. 3
n	path length in direction of $\bar{e}_2$ along intersection of η stream surface and φ potential surface, fig. 3
$\bar{n}$	unit vector normal to surface
$P_1, P_2, \ldots, P_{12}$	parameters given by eqs. (21g), (22g), and (23g)
p_U	path length along perimeter of upstream boundary, fig. 11
Q	ln q
q	velocity
$\bar{q}$	velocity vector, $\bar{e}_1 q$, fig. 3 and eq. (1b)
R	gas constant, J/(kg)(K)
$\bar{R}$	defined by eqs. (C2) and (C4)
$\mathfrak{R}$	residual error, eq. (28e)
r	polar coordinate
$\bar{r}$	position vector in physical space
r_U, θ'_U	polar coordinates on upstream boundary, fig. 12 and eq. (30g)
s	path length along streamline in direction of $\bar{e}_1$; or entropy, J/(kg)(K)
T	absolute temperature, K
u, v	curvilinear coordinates

u, v, w	components of velocity q in directions of $\bar{i}$, $\bar{j}$, and $\bar{k}$, respectively
V	volume
x, y, z	Cartesian coordinates in physical space
x_i	dummy variable
α, β, γ	angles of direction cosines in x, y, z-space, fig. 1
γ	ratio of specific heats; or geodesic curvature
ϵ	error
η	stream function, eqs. (6c)
θ	angle with which ψ and η stream surfaces intersect on potential surface, fig. 3 and eqs. (8b) and (8c)
θ'	polar coordinate
ρ	local density of fluid, eq. (4d)
φ	velocity potential, eqs. (5d)
φ, ψ, η	curvilinear coordinates in physical x, y, z-space or coordinates of transformed φ, ψ, η-space
ψ	stream function, eqs. (6c)
∇	vector differential operator, eqs. (5b) and (12a)
∇_S	vector differential operator on surface
$\times$	cross-product operator of two vectors
$\cdot$	dot-product operator of two vectors
Subscripts:	
C	cut line or surface cut
D	downstream boundary
max	maximum
min	minimum
o	total, or stagnation, condition
S	surface
U	upstream boundary
x	any grid point on a potential surface in φ, ψ, η-space

0, 1, . . ., 6	grid points in finite-difference star, fig. 10
1, 2, 3	variables or components of variables associated with directions of $\bar{e}_1$, $\bar{e}_2$, and $\bar{e}_3$, respectively
+, -	positive and negative directions, respectively, from central grid point in relaxation star, eq. (28a)
*	dimensional quantity

THEORY OF DESIGN METHOD

The theory of the design method is developed in this section. After preliminary considerations, the governing, second-order partial-differential equation for distribution of velocity in transformed φ, ψ, η-space is developed; additional equations, making use of results from the solution of the governing equation, are then developed for construction of the corresponding flow field in physical x, y, z-space.

Preliminary Considerations

The purpose of this design method is to determine the boundary shape of the potential flow field, in three-dimensional x, y, z-space, for which field the distribution of velocity everywhere on the boundary is as specified. This distribution of velocity is specified by $q(s)$, where s is distance along streamlines on the boundary. But, for potential flow, the velocity potential $\varphi(s)$ varies along each streamline according to the well-known relation (see eq. (5f))

$$\varphi(s) = \int q(s)ds$$

As a result, the prescribed distributions of velocity $q(s)$ on the physical boundary, of unknown shape, become prescribed distributions of velocity $q(\varphi)$ along the known curvilinear coordinate φ. If two additional curvilinear coordinates $\psi(x, y, z)$ and $\eta(x, y, z)$, related to the streamlines, can be determined, then the shape of the flow field in transformed φ, ψ, η-space is known, as is the prescribed velocity $q(s, \psi, \eta) = q(\varphi, \psi, \eta)$ on its boundary. The distribution of q throughout the flow field in φ, ψ, η-space can then be determined by a governing, partial-differential equation, and, from this distribution, the coordinates of the flow field, including the physical shape of boundary, can be computed in x, y, z-space. In this subsection, the general curvilinear φ, ψ, η-coordinates in x, y, z-space, which become Cartesian coordinates in φ, ψ, η-space, are identified.

Problem statement. - Given the shape of the upstream boundary surface and the distribution of the velocity q as a function of the distance s along streamlines on the surface of a three-dimensional, potential flow field, find the shape of the field.

Assumptions. - The flow is assumed to be steady and irrotational. The fluid is incompressible or subsonic-compressible. (Although, in regions of limited extent, supersonic velocities can probably be accommodated.)

Flow field in physical x,y,z-space. - A steady-flow field in x,y,z-space is defined by the spatial distribution of the velocity vector $\bar{q}$ and of the associated physical properties of the fluid. The local velocity vector $\bar{q}$ is given by its magnitude q and by a unit vector $\bar{e}_1$ in the direction of $\bar{q}$. This direction is tangent to the streamline, and, therefore, parallel to the elemental vector distance $\bar{e}_1 ds$ along the streamline. As shown in figure 1, at any point x,y,z, the direction of $\bar{e}_1$, and thus of $\bar{e}_1 ds$ and $\bar{e}_1 q$, is given by the direction cosines: $\cos \alpha_1$, $\cos \beta_1$, and $\cos \gamma_1$. Thus, if $\bar{i}$, $\bar{j}$, and $\bar{k}$ are unit vectors in the direction of x, y, and z, respectively,

$$\bar{e}_1 = \bar{i} \cos \alpha_1 + \bar{j} \cos \beta_1 + \bar{k} \cos \gamma_1 \tag{1a}$$

so that

$$\bar{q} = \bar{e}_1 q = \bar{i}u + \bar{j}v + \bar{k}w \tag{1b}$$

where u, v, and w are the velocity components in the x-, y-, and z-directions, respectively. Thus

$$\left.\begin{aligned} u &= q \cos \alpha_1 \\ v &= q \cos \beta_1 \\ w &= q \cos \gamma_1 \end{aligned}\right\} \tag{1c}$$

Likewise, for ds,

$$\left.\begin{aligned} dx &= ds \cos \alpha_1 \\ dy &= ds \cos \beta_1 \\ dz &= ds \cos \gamma_1 \end{aligned}\right\} \tag{1d}$$

from which it follows that

$$\cos^2 \alpha_1 + \cos^2 \beta_1 + \cos^2 \gamma_1 = 1 \tag{1e}$$

Density ρ. - For an incompressible fluid, the mass density ρ is constant, it does not affect the configuration of the flow field, and it, therefore, does not enter into the theory of the design method. For pure substances in the vapor phase only, that is, a real gas or a mixture of real gases, the static mass density ρ is a function of any two independent thermodynamic properties, of which at least one must be affected by the velocity q. It is convenient to select entropy s and static enthalpy h for these two properties. The static enthalpy is then related to the constant stagnation enthalpy h_o by

$$h = h_o - \frac{q^2}{2} \tag{2a}$$

and, for the irrotational motion of this design theory, the entropy s is constant. (More precisely, in the absence of external forces, and neglecting viscosity and heat conduction or radiation, Crocco's equation (ref. 4) shows that the flow field is irrotational, and, therefore, potential, if the entropy s and the total enthalpy h_o are constant.)

For perfect gases with constant entropy, the static mass density is related to the velocity and to the stagnation mass density ρ_o by

$$\rho = \rho_o \left(1 - \frac{\gamma - 1}{2} \frac{q^2}{\gamma R T_o}\right)^{1/(\gamma-1)} \tag{2b}$$

where the constants γ, R, and T_o are the ratio of specific heats, the gas constant, and the stagnation temperature, respectively.

Mach number M. - The local Mach number M is the velocity q divided by the local speed of sound c. Thus

$$M = \frac{q}{c} \tag{3a}$$

where

$$c^2 = \left(\frac{dp}{d\rho}\right)_{\text{isentropic}} \tag{3b}$$

Thus, from equations (3a) and (3b), for real gases,

$$M = \frac{q}{\sqrt{\left(\frac{dp}{d\rho}\right)_{isentropic}}} \tag{3c}$$

For a perfect gas,

$$\left(\frac{dp}{d\rho}\right)_{isentropic} = \gamma RT \tag{3d}$$

so that, from equations (3a), (3b), and (3d),

$$M = \frac{q}{\sqrt{\gamma RT}} \tag{3e}$$

where the local static temperature T is related to the constant stagnation temperature T_o by

$$T = T_o\left(1 - \frac{\gamma - 1}{2}\frac{q^2}{\gamma RT_o}\right) \tag{3f}$$

The local Mach number M is of critical interest in application of the design method to compressible flow fields, because the maximum velocity in the field, which velocity always occurs on the boundary and is, therefore, easily controlled, should normally be subsonic. Small local regions of supersonic flow can usually be accommodated, but strictly speaking, the fundamental character of the flow is different; the governing partial-differential equation changes from an elliptic to a hyperbolic type.

Nondimensional forms. - From this point on, it is convenient to treat all variables as nondimensional. Thus linear dimensions, such as x, y, z, and s, are normalized by the square root of the upstream boundary area $A_{U,*}$ in x, y, z-space:

$$x = \frac{x_*}{\sqrt{A_{U,*}}}, \text{ etc.} \tag{4a}$$

in which the subscript $*$ indicates a dimensional quantity. The velocity q and its components u, v, and w are normalized by the uniform velocity $q_{U,*}$ at the upstream boundary:

$$q = \frac{q_*}{q_{U,*}}, \text{ etc.} \tag{4b}$$

And the density ρ is normalized by the constant static density $\rho_{U,*}$ at the upstream boundary:

$$\rho = \frac{\rho_*}{\rho_{U,*}} \tag{4c}$$

Thus, for incompressible flow, the density is 1.0, and, for compressible flow of a perfect gas, from equation (2b), the density becomes

$$\rho = \left(\frac{1 - kq^2}{1 - k}\right)^{1/(\gamma-1)} \tag{4d}$$

where q is the nondimensional velocity, and

$$k = \frac{\gamma - 1}{2}\left(\frac{q_U^2}{\gamma R T_o}\right)_* \tag{4e}$$

Also, for a perfect gas, from equations (3e) and (3f), the Mach number M, expressed in terms of q, becomes

$$M = \sqrt{\frac{2}{\gamma - 1}\,\frac{kq^2}{1 - kq^2}} \tag{4f}$$

from which, at the upstream boundary where M is M_U and q is 1.0,

$$k = \frac{\frac{\gamma - 1}{2} M_U^2}{1 + \frac{\gamma - 1}{2} M_U^2} \tag{4g}$$

so that k is zero when M_U is zero, that is, when the flow is incompressible. Equation (4g) determines k for a specified value of M_U.

Velocity potential function $\varphi(x, y, z)$. - For irrotational flow,

$$\nabla \times \bar{q} = 0 \tag{5a}$$

where the vector differential operator ∇, expressed in terms of x, y, z-coordinates, is given by

$$\nabla = \bar{i}\frac{\partial}{\partial x} + \bar{j}\frac{\partial}{\partial y} + \bar{k}\frac{\partial}{\partial z} \tag{5b}$$

so that, from equation (1b),

$$\left.\begin{aligned} \frac{\partial w}{\partial y} - \frac{\partial v}{\partial z} &= 0 \\ \frac{\partial u}{\partial z} - \frac{\partial w}{\partial x} &= 0 \\ \frac{\partial v}{\partial x} - \frac{\partial u}{\partial y} &= 0 \end{aligned}\right\} \tag{5c}$$

From equations (5c), it follows that a velocity potential function $\varphi(x, y, z)$ exists in the flow field such that

$$\left.\begin{aligned} u &= \frac{\partial \varphi}{\partial x} \\ v &= \frac{\partial \varphi}{\partial y} \\ w &= \frac{\partial \varphi}{\partial z} \end{aligned}\right\} \tag{5d}$$

The existence of $\varphi(x, y, z)$ is confirmed by substitution of equations (5d) into equations (5c). Surfaces of constant φ in x, y, z-space are potential surfaces.

Because $\varphi(x, y, z)$ is a continuously differentiable point function of x, y, and z within the boundary of the flow field,

$$d\varphi = \frac{\partial \varphi}{\partial x}dx + \frac{\partial \varphi}{\partial y}dy + \frac{\partial \varphi}{\partial z}dz \tag{5e}$$

or, from equations (1c), (1d), and (1e), for an elemental distance ds along a streamline,

$$\frac{d\varphi}{ds} = q \tag{5f}$$

Equation (5f) is the result of irrotational flow.

Finally, from equations (5b) and (5d),

$$\nabla\varphi = \bar{i}\frac{\partial\varphi}{\partial x} + \bar{j}\frac{\partial\varphi}{\partial y} + \bar{k}\frac{\partial\varphi}{\partial z}$$

$$= \bar{i}u + \bar{j}v + \bar{k}w$$

or, from equation (1b),

$$\nabla\varphi = \bar{q} = \bar{e}_1 q \tag{5g}$$

Because $\nabla\varphi$, the vector gradient of φ, is everywhere normal to surfaces of constant φ, the velocity vector $\bar{q}$, which from equation (5g) is equal to $\nabla\varphi$, must also be normal to the surfaces of constant φ, as shown in figure 2.

Stream functions $\psi(x, y, z)$ and $\eta(x, y, z)$. - For steady, compressible flow, the continuity condition is

$$\nabla \cdot (\rho\bar{q}) = 0 \tag{6a}$$

so that, from equations (1b) and (5b),

$$\frac{\partial(\rho u)}{\partial x} + \frac{\partial(\rho v)}{\partial y} + \frac{\partial(\rho w)}{\partial z} = 0 \tag{6b}$$

where, for incompressible flow, the density ρ is 1.0. From equation (6b), it follows that two stream functions, $\psi(x, y, z)$ and $\eta(x, y, z)$, exist in the flow field such that (ref. 3)

$$\left.\begin{aligned} \rho u &= \frac{\partial\psi}{\partial y}\frac{\partial\eta}{\partial z} - \frac{\partial\psi}{\partial z}\frac{\partial\eta}{\partial y} \\ \rho v &= \frac{\partial\psi}{\partial z}\frac{\partial\eta}{\partial x} - \frac{\partial\psi}{\partial x}\frac{\partial\eta}{\partial z} \\ \rho w &= \frac{\partial\psi}{\partial x}\frac{\partial\eta}{\partial y} - \frac{\partial\psi}{\partial y}\frac{\partial\eta}{\partial x} \end{aligned}\right\} \tag{6c}$$

The existence of $\psi(x, y, z)$ and $\eta(x, y, z)$ is confirmed by substitution of equations (6c) into equation (6b). Surfaces of constant ψ and surfaces of constant η are stream surfaces in x, y, z-space.

Finally, from the cross product of the gradients of ψ and η,

$$\nabla\psi \times \nabla\eta = \left(\bar{i}\frac{\partial\psi}{\partial x} + \bar{j}\frac{\partial\psi}{\partial y} + \bar{k}\frac{\partial\psi}{\partial z}\right) \times \left(\bar{i}\frac{\partial\eta}{\partial x} + \bar{j}\frac{\partial\eta}{\partial y} + \bar{k}\frac{\partial\eta}{\partial z}\right)$$

$$= \begin{vmatrix} \bar{i} & \bar{j} & \bar{k} \\ \frac{\partial\psi}{\partial x} & \frac{\partial\psi}{\partial y} & \frac{\partial\psi}{\partial z} \\ \frac{\partial\eta}{\partial x} & \frac{\partial\eta}{\partial y} & \frac{\partial\eta}{\partial z} \end{vmatrix}$$

$$= \bar{i}\left(\frac{\partial\psi}{\partial y}\frac{\partial\eta}{\partial z} - \frac{\partial\psi}{\partial z}\frac{\partial\eta}{\partial y}\right) + \bar{j}\left(\frac{\partial\psi}{\partial z}\frac{\partial\eta}{\partial x} - \frac{\partial\psi}{\partial x}\frac{\partial\eta}{\partial z}\right) + \bar{k}\left(\frac{\partial\psi}{\partial x}\frac{\partial\eta}{\partial y} - \frac{\partial\psi}{\partial y}\frac{\partial\eta}{\partial x}\right)$$

or, from equations (1b), (5g), and (6c),

$$\left.\begin{aligned} \nabla\psi \times \nabla\eta &= \bar{i}(\rho u) + \bar{j}(\rho v) + \bar{k}(\rho w) \\ &= \rho\bar{q} \\ &= \rho\bar{e}_1 q \\ &= \rho\nabla\varphi \end{aligned}\right\} \qquad (6d)$$

From equation (6d), the gradients $\nabla\psi$ and $\nabla\eta$, which are normal to the stream surfaces of constant ψ and of constant η, respectively, are normal to $\bar{q}$ and $\nabla\varphi$. It follows directly, as shown in figure 3, that the gradients of ψ and of η lie on surfaces of constant φ and, therefore, that stream surfaces of constant ψ or of constant η are normal to potential surfaces of constant φ. (Also see appendix A.) Because the stream surfaces of constant ψ or of constant η are both normal to potential surfaces of constant φ, their intersections are also normal to surfaces of constant φ and are, therefore, parallel to the velocity vector $\bar{q}$. Thus the intersections of stream surfaces of constant ψ with stream surfaces of constant η are streamlines, and the values of ψ and η along a streamline are constant. In a similar fashion, the intersections of adjacent stream surfaces of constant ψ and $\psi + \delta\psi$ with adjacent stream surfaces of constant η and $\eta + \delta\eta$ define stream tubes, as shown in figure 4. Thus fluid does not flow across stream surfaces of constant ψ and η; these stream surfaces are, in effect, generated by fluid lines of connected particles on the upstream boundary that pass downstream through the flow field and thereby divide it. Because the selected (input) shape and orientation of these fluid lines at the upstream boundary are somewhat arbi-

trary, the shape of the resulting stream surfaces and the angle θ (fig. 3) with which the stream surfaces of constant ψ intersect stream surfaces of constant η (measured on potential surfaces of constant φ) vary with fluid line selection for the same boundary shape of flow field in x, y, z-space.

Curvilinear φ, ψ, η-coordinates in x, y, z-space. - The two families of stream surfaces of constant ψ and of constant η together with the family of potential surfaces of constant φ form a curvilinear φ, ψ, η-coordinate system for the flow field in x, y, z-space. On stream surfaces of constant ψ (fig. 3), there is a coordinate system of η and φ lines. For these η, φ-surfaces of constant ψ, the η- and φ-coordinate lines are orthogonal, as shown previously by equation (6d). (Also see appendix A.) Likewise, on stream surfaces of constant η (fig. 3), there is a coordinate system of φ and ψ lines. For these φ, ψ-surfaces of constant η, the φ- and ψ-coordinate lines are again orthogonal, as shown previously by equation (6d). (Also see appendix A.) On the potential surfaces of constant φ (fig. 3), there is a coordinate system of ψ and η lines. For these ψ, η-surfaces of constant φ, however, the ψ- and η-coordinates are not generally orthogonal, but intersect at an angle $\theta(\varphi, \psi, \eta)$ that varies with location in the flow field. (See fig. 3 and appendix A.) Thus, in this one respect, the curvilinear φ, ψ, η-coordinates are not orthogonal in x, y, z-space.

Unit vectors $\bar{e}_1$, $\bar{e}_2$, and $\bar{e}_3$. - At every point of the flow field in x, y, z-space, the unit vectors $\bar{e}_1$, $\bar{e}_2$, and $\bar{e}_3$ (fig. 3) are tangent to intersections of the stream surfaces and the potential surface. The unit vector $\bar{e}_1$ is tangent to the intersections of ψ and η stream surfaces and points in the direction of increasing distance s and of increasing velocity potential φ along the intersections (which are streamlines). This unit vector is defined in terms of its direction cosines by (also see eq. (1a))

$$\bar{e}_1 = \bar{i} \cos \alpha_1 + \bar{j} \cos \beta_1 + \bar{k} \cos \gamma_1 \tag{7a}$$

where, from equations (1d),

$$\left.\begin{aligned} \cos \alpha_1 &= \frac{dx}{ds} \\ \cos \beta_1 &= \frac{dy}{ds} \\ \cos \gamma_1 &= \frac{dz}{ds} \end{aligned}\right\} \tag{7b}$$

in which ds (fig. 3) is elemental distance along the intersections, and dx, dy, and dz are corresponding elemental distances in the x, y, z-coordinate directions.

The unit vector $\bar{e}_2$ is tangent to the intersections of η stream surfaces and φ potential surfaces and points in the direction of increasing distance n and of increasing stream function ψ along these intersections. This unit vector is defined in terms of its direction cosines by

$$\bar{e}_2 = \bar{i} \cos \alpha_2 + \bar{j} \cos \beta_2 + \bar{k} \cos \gamma_2 \tag{7c}$$

where

$$\left.\begin{aligned} \cos \alpha_2 &= \frac{dx}{dn} \\ \cos \beta_2 &= \frac{dy}{dn} \\ \cos \gamma_2 &= \frac{dz}{dn} \end{aligned}\right\} \tag{7d}$$

in which dn (fig. 3) is elemental distance along the intersections.

The unit vector $\bar{e}_3$ is tangent to the intersections of φ potential surfaces and ψ stream surfaces and points in the direction of increasing distance m and of increasing stream function η along these intersections. This unit vector is defined in terms of its direction cosines by

$$\bar{e}_3 = \bar{i} \cos \alpha_3 + \bar{j} \cos \beta_3 + \bar{k} \cos \gamma_3 \tag{7e}$$

where

$$\left.\begin{aligned} \cos \alpha_3 &= \frac{dx}{dm} \\ \cos \beta_3 &= \frac{dy}{dm} \\ \cos \gamma_3 &= \frac{dz}{dm} \end{aligned}\right\} \tag{7f}$$

in which dm (fig. 3) is elemental distance along the intersections.

The unit vectors $\bar{e}_1$, $\bar{e}_2$, and $\bar{e}_3$ are tangent to the curvilinear coordinate lines and pointed in the directions of increasing φ, ψ, and η, respectively.

Angle θ. - Because the ψ and η stream surfaces are normal to the φ potential surface, the unit vectors $\bar{e}_2$ and $\bar{e}_3$ are normal to the unit vector $\bar{e}_1$. Thus

$$\left.\begin{aligned} \bar{e}_1 \cdot \bar{e}_2 &= 0 \\ \bar{e}_3 \cdot \bar{e}_1 &= 0 \end{aligned}\right\} \tag{8a}$$

And, because the two stream surfaces intersect at an angle $\theta(\varphi, \psi, \eta)$ (fig. 3) on the ψ, η-potential surface,

$$\bar{e}_2 \cdot \bar{e}_3 = \cos \theta(\varphi, \psi, \eta) \tag{8b}$$

From equations (7c), (7e), and (8b),

$$\cos \theta(\varphi, \psi, \eta) = \cos \alpha_2 \cos \alpha_3 + \cos \beta_2 \cos \beta_3 + \cos \gamma_2 \cos \gamma_3 \tag{8c}$$

(Also see appendix A.)

The angle θ is a major parameter in the governing, partial-differential equation of the design method. From figure 4 (and fig. 6), it can be seen that the range of θ values is limited to

$$0 < \theta < 180^{\circ} \tag{8d}$$

Otherwise the area of the stream tube would become negative.

Gradients $\nabla\varphi$, $\nabla\psi$, and $\nabla\eta$. - The gradients of φ, ψ, and η in x, y, z-space are differential invariants that can be expressed in terms of any convenient coordinate system in x, y, z-space, for example, in terms of the natural coordinates s, n, and m (fig. 3). The gradient $\nabla\varphi$, which is normal to potential surfaces of constant φ, is in the direction of $\bar{e}_1$ and has the magnitude $d\varphi/ds$. Thus

$$\nabla\varphi = \bar{e}_1 \frac{d\varphi}{ds} \tag{9a}$$

which also follows from equations (5f) and (5g).

The gradients $\nabla\psi$ and $\nabla\eta$, which lie on potential surfaces (fig. 3) and are normal to stream surfaces of constant ψ and to stream surfaces of constant η, respectively, have the directions $\bar{e}_3 \times \bar{e}_1$ and $\bar{e}_1 \times \bar{e}_2$, respectively, as shown in figure 5. Also, from figure 5, the magnitudes of these gradients are $(1/\sin\theta)d\psi/dn$ and $(1/\sin\theta)d\eta/dm$, respectively, where $\sin\theta$ appears because $d\psi/dn$ and $d\eta/dm$ are in the directions of $\bar{e}_2$ and $\bar{e}_3$, respectively. Thus

$$\nabla\psi = \bar{e}_3 \times \bar{e}_1 \frac{1}{\sin\theta} \frac{d\psi}{dn} \tag{9b}$$

$$\nabla\eta = \bar{e}_1 \times \bar{e}_2 \frac{1}{\sin\theta} \frac{d\eta}{dm} \tag{9c}$$

These gradients are required to transform the fundamental equations of flow from x, y, z-space to φ, ψ, η-space.

From equations (9b) and (9c),

$$\nabla\psi \times \nabla\eta = \left(\bar{e}_3 \times \bar{e}_1\right) \times \left(\bar{e}_1 \times \bar{e}_2\right) \frac{1}{\sin^2\theta} \frac{d\psi}{dn} \frac{d\eta}{dm}$$

where, from figure 5,

$$\left(\bar{e}_3 \times \bar{e}_1\right) \times \left(\bar{e}_1 \times \bar{e}_2\right) = \bar{e}_1 \sin\theta$$

so that, from equation (6d),

$$\bar{e}_1 \rho q = \bar{e}_1 \frac{1}{\sin\theta} \frac{d\psi}{dn} \frac{d\eta}{dm}$$

or

$$d\psi\, d\eta = \rho q (dn\, dm \sin\theta) \tag{9d}$$

Equation (9d) is the result of continuity, where $\rho q (dn\, dm \sin\theta)$ is the differential mass flow rate across the elemental area $(dn\, dm \sin\theta)$ bounded by adjacent ψ and η lines of differential magnitude $d\psi$ and $d\eta$, respectively, on the potential surface in figure 6.

From equations (5f) and (9d), it follows that

$$\frac{d\varphi\, d\psi\, d\eta}{dV} = \rho q^2 \tag{9e}$$

where, from figure 7, the elemental volume dV, bounded by adjacent potential and stream surfaces of differential magnitude $d\varphi$, $d\psi$, and $d\eta$, is given by

$$dV = ds (dn\, dm \sin\theta) \tag{9f}$$

Thus, from equation (9e), for given values of $d\varphi$, $d\psi$, and $d\eta$, the smaller the elemental volume dV, the greater ρq^2.

From figure 5, the cross products involving $\bar{e}_1$ in equations (9b) and (9c) can be expressed in terms of the unit vectors $\bar{e}_2$ and $\bar{e}_3$ lying on potential surfaces. Thus

$$\bar{e}_3 \times \bar{e}_1 = \frac{1}{\sin\theta}\left(\bar{e}_2 - \bar{e}_3 \cos\theta\right) \tag{9g}$$

$$\bar{e}_1 \times \bar{e}_2 = \frac{1}{\sin\theta}\left(\bar{e}_3 - \bar{e}_2 \cos\theta\right) \tag{9h}$$

from which, equations (9b) and (9c) become

$$\nabla\psi = \frac{1}{\sin^2\theta}\left(\bar{e}_2 - \bar{e}_3 \cos\theta\right)\frac{d\psi}{dn} \tag{9i}$$

$$\nabla\eta = \frac{1}{\sin^2\theta}\left(\bar{e}_3 - \bar{e}_2 \cos\theta\right)\frac{d\eta}{dm} \tag{9j}$$

Parameters A and B. - In the development of the design method, it is convenient to introduce two parameters, A and B, which are defined by

$$A = \rho \frac{dn}{d\psi} \sin\theta \tag{10a}$$

$$B = \rho \frac{dm}{d\eta} \sin\theta \tag{10b}$$

In equation (10a), and as shown in figure 8, dn sin θ is the local thickness of the differential stream lamina bounded by the adjacent stream surfaces of constant ψ and of constant $\psi + d\psi$. The parameter A, which is this thickness multiplied by the local density, is, therefore, a measure of the local mass-flow capacity of the stream lamina for any given value of the local velocity q. Likewise, from equation (10b) and figure 8, the parameter B is a measure of the local mass-flow capacity of the differential stream lamina bounded by the adjacent stream surfaces of constant η and of constant $\eta + d\eta$.

From equations (10a) and (10b), for equal values of $d\psi$ and $d\eta$,

$$\frac{A}{B} = \left(\frac{dn}{dm}\right)_{d\psi=d\eta} \tag{10c}$$

which is the ratio of sides for the elemental flow area in figure 6. Also, from equations (10a) and (10b),

$$AB = \rho^2 \frac{dn}{d\psi} \frac{dm}{d\eta} \sin^2\theta$$

or, from the continuity equation (9d),

$$AB = \frac{\rho \sin \theta}{q} \tag{10d}$$

From equations (9d) and (10b),

$$\frac{d\psi}{dn} = qB \tag{10e}$$

and equation (9i) becomes

$$\nabla\psi = \frac{qB}{\sin^2\theta}\left(\bar{e}_2 - \bar{e}_3 \cos\theta\right) \tag{10f}$$

Likewise, from equations (9d) and (10a),

$$\frac{d\eta}{dm} = qA \tag{10g}$$

and equation (9j) becomes

$$\nabla\eta = \frac{qA}{\sin^2\theta}\left(\bar{e}_3 - \bar{e}_2 \cos\theta\right) \tag{10h}$$

Equations (10f) and (10h) are final forms for the gradients of ψ and η, respectively. The gradient of φ is given by equation (5g).

In summary, from equations (5f), (10e), and (10g),

$$\left.\begin{aligned} \frac{d\varphi}{ds} &= q \qquad (5f) \\ \frac{d\psi}{dn} &= qB \qquad (10e) \\ \frac{d\eta}{dm} &= qA \qquad (10g) \end{aligned}\right\} \tag{10i}$$

The first of these equations is the result of irrotational fluid motion; the second and third result from continuity.

Flow field in transformed φ, ψ, η-space. - The upstream and downstream boundaries of the flow field in transformed φ, ψ, η-space can be, for convenience, plane surfaces of constant φ. If the value of φ at the upstream boundary is taken as zero, the downstream value φ_D is, from equation (5f),

$$\varphi_D = \int_0^{s_D} q(s)ds \tag{11}$$

where the subscript D refers to the downstream boundary, and q(s) is the prescribed distribution of velocity q as a function of distance s along streamlines on the lateral surface of the flow field. If the downstream surface is a plane of constant φ_D, these prescribed distributions of q(s) must be such that the integral in equation (11) is the same for all these streamlines.

The boundary shape of the flow field on planes of constant φ in φ, ψ, η-space depends on (1) the specified shape of the upstream boundary surface in x, y, z-space and (2) the somewhat-arbitrary, specified shape and orientation of constant ψ and constant η lines on that upstream boundary. However, whatever the shape of the boundary on the upstream φ-plane in φ, ψ, η-space, the same shape exists for all planes of constant φ, because the paired values of ψ and η for each streamline on the lateral boundary remain constant. Thus the flow field in φ, ψ, η-space is a right cylinder (fig. 9) or a rectangular parallelepiped.

Outline of method. - When q is specified as a function of s along streamlines on the lateral surfaces of the flow field, then, from equation (5f) and with uniform velocities on the upstream and downstream planes, the velocity q is known everywhere on the boundary in φ, ψ, η-space. For these known boundary values of q, a governing, partial-differential equation, derived from the laws of potential flow expressed in curvilinear coordinates, is developed for the distribution of q within the flow field in φ, ψ, η-space. And from this distribution of q within the field, auxiliary equations are used to compute flow directions and the shape of the flow field in x, y, z-space.

Governing, Partial-Differential Equation for Distribution of Velocity in Transformed φ, ψ, η-Space

The governing, partial-differential equation for the distribution of velocity q in transformed φ, ψ, η-space is developed from the conditions of continuity and irrotationality for three-dimensional, compressible flow. This general equation is then reduced for the special cases of (1) incompressible flow, (2) plane two-dimensional flow, and (3) axisymmetric flow.

Vector differential operator ∇. - Expressed in terms of the curvilinear φ, ψ, η-coordinates, the vector differential operator ∇ is given by

$$\nabla = \nabla\varphi \frac{\partial}{\partial\varphi} + \nabla\psi \frac{\partial}{\partial\psi} + \nabla\eta \frac{\partial}{\partial\eta} \tag{12a}$$

where the vector gradients $\nabla\varphi$, $\nabla\psi$, and $\nabla\eta$ are given by equations (5g), (10f), and (10h), respectively. Thus

$$\nabla = \bar{e}_1 q \frac{\partial}{\partial\varphi} + \left(\bar{e}_2 - \bar{e}_3 \cos\theta\right) \frac{qB}{\sin^2\theta} \frac{\partial}{\partial\psi} + \left(\bar{e}_3 - \bar{e}_2 \cos\theta\right) \frac{qA}{\sin^2\theta} \frac{\partial}{\partial\eta} \tag{12b}$$

Equation (12b) gives the vector differential operator ∇ in terms of (1) the partial differentials with respect to φ, ψ, and η and (2) the unit vectors $\bar{e}_1$, $\bar{e}_2$, and $\bar{e}_3$.

Irrotationality condition. - For irrotational flow, the vorticity of the velocity vector is zero. Thus

$$\nabla \times \bar{q} = 0 \tag{13a}$$

or, from equations (1b) and (12b),

$$\left[\bar{e}_1 \frac{\partial}{\partial\varphi} + \left(\bar{e}_2 - \bar{e}_3 \cos\theta\right) \frac{B}{\sin^2\theta} \frac{\partial}{\partial\psi} + \left(\bar{e}_3 - \bar{e}_2 \cos\theta\right) \frac{A}{\sin^2\theta} \frac{\partial}{\partial\eta}\right] \times \bar{e}_1 q = 0$$

so that, with (see fig. 5)

$$\frac{\bar{e}_2 - \bar{e}_3 \cos\theta}{\sin\theta} \times \bar{e}_1 = -\bar{e}_3 \tag{13b}$$

$$\frac{\bar{e}_3 - \bar{e}_2 \cos\theta}{\sin\theta} \times \bar{e}_1 = \bar{e}_2 \tag{13c}$$

the vector equation for zero vorticity is

$$\bar{e}_1 \times \frac{\partial \bar{e}_1}{\partial\varphi} - \frac{B}{\sin\theta} \bar{e}_3 \frac{\partial \ln q}{\partial\psi} + \frac{B}{\sin^2\theta} \left(\bar{e}_2 - \bar{e}_3 \cos\theta\right) \times \frac{\partial \bar{e}_1}{\partial\psi} + \frac{A}{\sin\theta} \bar{e}_2 \frac{\partial \ln q}{\partial\eta}$$

$$+ \frac{A}{\sin^2\theta} \left(\bar{e}_3 - \bar{e}_2 \cos\theta\right) \times \frac{\partial \bar{e}_1}{\partial\eta} = 0 \tag{13d}$$

Because the vectors $\partial\bar{e}_1/\partial\varphi$, $\partial\bar{e}_1/\partial\psi$, and $\partial\bar{e}_1/\partial\eta$ are normal to $\bar{e}_1$, they lie on the plane tangent to the φ surface, as do the unit vectors $\bar{e}_2$ and $\bar{e}_3$ (see fig. 5). Thus the first, second, and fourth terms of equation (13d) are vectors that lie on the tangent plane and are normal to $\bar{e}_1$; the third and fifth terms are vectors that are normal to the tangent plane and, thus, parallel to $\bar{e}_1$. Therefore the vorticity component normal to the η surface, which vorticity component is zero, is obtained from the dot product of the first, second, and fourth terms with the unit vector $\bar{e}_1 \times \bar{e}_2$, which vector is normal to that surface (see figs. 3 and 5). Thus

$$\left(\bar{e}_1 \times \frac{\partial \bar{e}_1}{\partial \varphi} - \frac{B}{\sin\theta}\bar{e}_3 \frac{\partial \ln q}{\partial \psi} + \frac{A}{\sin\theta}\bar{e}_2 \frac{\partial \ln q}{\partial \eta}\right) \cdot \left(\bar{e}_1 \times \bar{e}_2\right) = 0$$

which, from equation (9h) and from page 18 of reference 5, reduces to

$$\bar{e}_2 \cdot \frac{\partial \bar{e}_1}{\partial \varphi} - B \frac{\partial \ln q}{\partial \psi} = 0 \tag{13e}$$

Equation (13e) is the first of three scalar equations resulting from the irrotationality condition. Each term in this equation is equal to $1/q$ times the local geodesic curvature γ_1 of the φ-coordinate line on the η stream surface in x,y,z-space (eq. (B7), appendix B).

Likewise the vorticity component normal to the ψ surface, which vorticity component is zero, is obtained from the dot product of the first, second, and fourth terms in equation (13d) with the unit vector $\bar{e}_3 \times \bar{e}_1$, which vector is normal to that surface (see figs. 3 and 5). Thus

$$\left(\bar{e}_1 \times \frac{\partial \bar{e}_1}{\partial \varphi} - \frac{B}{\sin\theta}\bar{e}_3 \frac{\partial \ln q}{\partial \psi} + \frac{A}{\sin\theta}\bar{e}_2 \frac{\partial \ln q}{\partial \eta}\right) \cdot \left(\bar{e}_3 \times \bar{e}_1\right) = 0$$

which, from equation (9g) and from page 18 of reference 5, reduces to

$$A \frac{\partial \ln q}{\partial \eta} - \bar{e}_3 \cdot \frac{\partial \bar{e}_1}{\partial \varphi} = 0 \tag{13f}$$

Equation (13f) is the second of the three scalar equations resulting from the irrotationality condition. Each term in this equation is equal to $-1/q$ times the local geodesic curvature γ_1 of the φ-coordinate line on the ψ stream surface in x,y,z-space (eq. (B14), appendix B).

Finally, the vorticity component normal to the φ-surface, which vorticity component is zero, is obtained from the dot product of the third and fifth terms in equation (13d) with $\bar{e}_1$, which vector is normal to that surface. Thus

$$\left[\frac{B}{\sin^2\theta}\left(\bar{e}_2 - \bar{e}_3\cos\theta\right)\times\frac{\partial\bar{e}_1}{\partial\psi} + \frac{A}{\sin^2\theta}\left(\bar{e}_3 - \bar{e}_2\cos\theta\right)\times\frac{\partial\bar{e}_1}{\partial\eta}\right]\cdot\bar{e}_1 = 0$$

which, from equations (9g) and (9h) and from page 17 of reference 5, reduces to

$$B\bar{e}_3\cdot\frac{\partial\bar{e}_1}{\partial\psi} - A\bar{e}_2\cdot\frac{\partial\bar{e}_1}{\partial\eta} = 0 \tag{13g}$$

Equation (13g) is the third of the three scalar equations resulting from the irrotationality condition. Because $\bar{q}$ is normal to the φ-surface, this equation does not involve the velocity magnitude q. To determine the physical significance of this equation, consider the vector component itself, rather than its scalar value. The third and fifth terms of equation (13d), after equations (10f) and (10h) are introduced, become

$$\nabla\psi\times\frac{\partial\bar{e}_1}{\partial\psi} + \nabla\eta\times\frac{\partial\bar{e}_1}{\partial\eta} = \nabla_S\times\bar{e}_1 = 0 \tag{13h}$$

where $\nabla_S\times\bar{e}_1$ is the surface rotation of $\bar{e}_1$ on a constant φ-surface, here expressed in curvilinear ψ,η-coordinates. (Note that the gradients $\nabla\psi$ and $\nabla\eta$ both lie on the φ-surface.) Thus, from equation (13h), the surface rotation of the unit vector $\bar{e}_1$ normal to the φ-surface is zero. This condition is true for the unit vector normal to any surface (ref. 6, p. 208).

Surface rotation of normal unit vectors. - Similar to equation (13h), the surface rotation of the unit vector $\bar{e}_1\times\bar{e}_2$ normal to the η-surface is equal to zero. Thus

$$\nabla_S\times\left(\bar{e}_1\times\bar{e}_2\right) = \left(\nabla\varphi\frac{\partial}{\partial\varphi} + \nabla_S\psi\frac{\partial}{\partial\psi}\right)\times\left(\bar{e}_1\times\bar{e}_2\right) = 0 \tag{14a}$$

where $\nabla_S\psi$ is the surface gradient of ψ on the η-surface. (The spatial gradient $\nabla\varphi$ lies on the η-surface.) From equation (10e),

$$\nabla_S\psi = \bar{e}_2\frac{d\psi}{dn} = \bar{e}_2 qB \tag{14b}$$

Thus, from equations (5g), (14a), and (14b),

$$\bar{e}_1 \times \frac{\partial\left(\bar{e}_1 \times \bar{e}_2\right)}{\partial\varphi} + B\bar{e}_2 \times \frac{\partial\left(\bar{e}_1 \times \bar{e}_2\right)}{\partial\psi} = 0$$

Expanding the triple vector products and taking the dot product of the result in the direction of $e_1 \times e_2$ yield

$$\left(B\frac{\partial\bar{e}_1}{\partial\psi} - \frac{\partial\bar{e}_2}{\partial\varphi}\right) \cdot \left(\bar{e}_1 \times \bar{e}_2\right) = 0$$

or introducing equation (9h) gives

$$\bar{e}_3 \cdot \frac{\partial\bar{e}_2}{\partial\varphi} = B\left(\bar{e}_3 - \bar{e}_2 \cos\theta\right) \cdot \frac{\partial\bar{e}_1}{\partial\psi} \tag{14c}$$

In the same fashion, because the surface rotation of the unit vector $\bar{e}_3 \times \bar{e}_1$ normal to the ψ-surface is zero,

$$\bar{e}_2 \cdot \frac{\partial\bar{e}_3}{\partial\varphi} = A\left(\bar{e}_2 - \bar{e}_3 \cos\theta\right) \cdot \frac{\partial\bar{e}_1}{\partial\eta} \tag{14d}$$

Equations (14c) and (14d), which result from zero surface rotation of the unit vectors $\bar{e}_1 \times \bar{e}_2$ and $\bar{e}_3 \times \bar{e}_1$ normal to the η- and ψ-surfaces, respectively, can be combined as follows. From equation (8b) and the fact that $\sin^2\theta + \cos^2\theta = 1$,

$$\bar{e}_2 \cdot \frac{\partial\bar{e}_3}{\partial\varphi} + \bar{e}_3 \cdot \frac{\partial\bar{e}_2}{\partial\varphi} = -\frac{\sin^2\theta}{\cos\theta}\frac{\partial \ln \sin\theta}{\partial\varphi}$$

or, from equations (14c) and (14d),

$$\frac{B}{\sin^2\theta}\left(\bar{e}_2 - \bar{e}_3 \cos\theta\right) \cdot \frac{\partial\bar{e}_1}{\partial\psi} + \frac{A}{\sin^2\theta}\left(\bar{e}_3 - \bar{e}_2 \cos\theta\right) \cdot \frac{\partial\bar{e}_1}{\partial\eta} =$$

$$B\bar{e}_2 \cdot \frac{\partial\bar{e}_1}{\partial\psi} + A\bar{e}_3 \cdot \frac{\partial\bar{e}_1}{\partial\eta} + \frac{\partial \ln \sin\theta}{\partial\varphi} \tag{14e}$$

Equation (14e) is used later to simplify the continuity equation.

Continuity condition. - For steady, compressible flow, the divergence of the product of the velocity vector and the fluid density is zero. Thus

$$\nabla \cdot (\rho \bar{q}) = 0 \tag{15a}$$

or, from equations (1b) and (12b),

$$\bar{e}_1 \cdot \frac{\partial\left(\bar{e}_1 \rho q\right)}{\partial \varphi} + \frac{B}{\sin^2\theta}\left(\bar{e}_2 - \bar{e}_3 \cos\theta\right) \cdot \frac{\partial\left(\bar{e}_1 \rho q\right)}{\partial \psi} + \frac{A}{\sin^2\theta}\left(\bar{e}_3 - \bar{e}_2 \cos\theta\right) \cdot \frac{\partial\left(\bar{e}_1 \rho q\right)}{\partial \eta} = 0$$

which expands to give

$$\frac{\partial \ln q}{\partial \varphi} + \frac{\partial \ln \rho}{\partial \varphi} + \frac{B}{\sin^2\theta}\left(\bar{e}_2 - \bar{e}_3 \cos\theta\right) \cdot \frac{\partial \bar{e}_1}{\partial \psi} + \frac{A}{\sin^2\theta}\left(\bar{e}_3 - \bar{e}_2 \cos\theta\right) \cdot \frac{\partial \bar{e}_1}{\partial \eta} = 0$$

Introducing equation (14e) gives the continuity equation in transformed φ, ψ, η-coordinates:

$$\frac{\partial \ln q}{\partial \varphi} + \frac{\partial \ln \rho}{\partial \varphi} + B\bar{e}_2 \cdot \frac{\partial \bar{e}_1}{\partial \psi} + A\bar{e}_3 \cdot \frac{\partial \bar{e}_1}{\partial \eta} + \frac{\partial \ln \sin\theta}{\partial \varphi} = 0 \tag{15b}$$

Surface divergence of flow in stream laminae. - In a steady, three-dimensional, compressible flow field, consider the fluid in a differential stream lamina bounded by adjacent stream surfaces of constant η and of constant $\eta + d\eta$. In general, the elemental thickness $dm \sin\theta$ (fig. 8) of this lamina varies from point to point on the η-surface of the lamina. From continuity, the surface divergence of the flow $\rho\bar{q}\, dm \sin\theta$ in the lamina is zero. Thus

$$\nabla_S \cdot (\rho \bar{q}\, dm \sin\theta) = 0 \tag{16a}$$

where, as in equation (14a),

$$\nabla_S = \nabla\varphi \frac{\partial}{\partial \varphi} + \nabla_S\psi \frac{\partial}{\partial \psi} \tag{16b}$$

so that, from equations (5g), (14b), and (16b), equation (16a) becomes

$$\left(\bar{e}_1 \frac{\partial}{\partial \varphi} + \bar{e}_2 B \frac{\partial}{\partial \psi}\right) \cdot (q\bar{e}_1 B\, d\eta) = 0$$

which, with $d\eta$ constant for the lamina, reduces to

$$B\bar{e}_2 \cdot \frac{\partial \bar{e}_1}{\partial \psi} = -\frac{\partial \ln q}{\partial \varphi} - \frac{\partial \ln B}{\partial \varphi} \tag{16c}$$

Likewise, for the flow in a differential stream lamina bounded by adjacent stream surfaces of constant ψ and of constant $\psi + d\psi$,

$$A\bar{e}_3 \cdot \frac{\partial \bar{e}_1}{\partial \eta} = -\frac{\partial \ln q}{\partial \varphi} - \frac{\partial \ln A}{\partial \varphi} \tag{16d}$$

Equations (16c) and (16d) are the continuity equations for flow in the two families of stream laminae. Each side of equation (16c) is equal to $1/q$ times the local geodesic curvature γ_2 of the ψ-coordinate line on the η stream surface in x, y, z-space (eq. (B8), appendix B); likewise each side of equation (16d) is equal to $-1/q$ times the local geodesic curvature γ_3 of the η-coordinate line on the ψ stream surface (eq. (B13), appendix B).

If equations (16c) and (16d) are entered into the general continuity equation (15b),

$$\frac{\partial \ln \rho}{\partial \varphi} - \frac{\partial \ln q}{\partial \varphi} - \frac{\partial \ln A}{\partial \varphi} - \frac{\partial \ln B}{\partial \varphi} + \frac{\partial \ln \sin \theta}{\partial \varphi} = 0$$

or

$$\frac{\rho \sin \theta}{qAB} = \text{constant}$$

where, from equation (10d), the constant is 1.

Governing differential equation. - The governing differential equation for the distribution of velocity q in φ, ψ, η-space is derived from the continuity equation (15b) and from the two equations for the irrotationality condition, equations (13e) and (13f).

As already observed, any three-dimensional, steady-flow field is defined by the spatial distribution of the velocity q and its direction $\bar{e}_1$, where, from equation (1a) and/or figure 1, the unit vector $\bar{e}_1$ is defined by the three angles α_1, β_1, and γ_1. From equation (1a), the three angles are related by

$$\bar{e}_1 \cdot \bar{e}_1 = 1 = \cos^2 \alpha_1 + \cos^2 \beta_1 + \cos^2 \gamma_1 \tag{17a}$$

Thus, when equation (17a) is taken into account, the flow field is defined by three unknowns: the velocity q and two flow angles. The solution, therefore, involves three equations. These equations are the continuity equation (15b) and the two equations for the irrotationality condition, equations (13e) and (13f). All three of these equations

involve partial derivatives of q and $\bar{e}_1$ only. After appropriate second partial derivatives are obtained, the three equations are combined to eliminate the second partial derivatives of $\bar{e}_1$.

Thus, from the continuity equation (15b), after the partial derivative with respect to φ is taken,

$$\frac{\partial^2 \ln q}{\partial \varphi^2} + \frac{\partial^2 \ln \rho}{\partial \varphi^2} + \frac{\partial^2 \ln \sin\theta}{\partial \varphi^2} + B \frac{\partial \ln B}{\partial \varphi} \bar{e}_2 \cdot \frac{\partial \bar{e}_1}{\partial \psi} + B \frac{\partial \bar{e}_2}{\partial \varphi} \cdot \frac{\partial \bar{e}_1}{\partial \psi} + B\bar{e}_2 \cdot \frac{\partial^2 \bar{e}_1}{\partial \varphi \, \partial \psi}$$

$$+ A \frac{\partial \ln A}{\partial \varphi} \bar{e}_3 \cdot \frac{\partial \bar{e}_1}{\partial \eta} + A \frac{\partial \bar{e}_3}{\partial \varphi} \cdot \frac{\partial \bar{e}_1}{\partial \eta} + A\bar{e}_3 \cdot \frac{\partial^2 \bar{e}_1}{\partial \varphi \, \partial \eta} = 0 \qquad (17b)$$

where, from the irrotationality equation (13e), after the partial derivative with respect to ψ is taken,

$$B\bar{e}_2 \cdot \frac{\partial^2 \bar{e}_1}{\partial \varphi \, \partial \psi} = -B \frac{\partial \bar{e}_2}{\partial \psi} \cdot \frac{\partial \bar{e}_1}{\partial \varphi} + B^2 \frac{\partial \ln B}{\partial \psi} \frac{\partial \ln q}{\partial \psi} + B^2 \frac{\partial^2 \ln q}{\partial \psi^2} \qquad (17c)$$

and where, from the irrotationality equation (13f), after the partial derivative with respect to η is taken,

$$A\bar{e}_3 \cdot \frac{\partial^2 \bar{e}_1}{\partial \varphi \, \partial \eta} = -A \frac{\partial \bar{e}_3}{\partial \eta} \cdot \frac{\partial \bar{e}_1}{\partial \varphi} + A^2 \frac{\partial \ln A}{\partial \eta} \frac{\partial \ln q}{\partial \eta} + A^2 \frac{\partial^2 \ln q}{\partial \eta^2} \qquad (17d)$$

Therefore, from equations (17b), (17c), and (17d), after equations (16c) and (16d) are introduced, the governing differential equation for ln q becomes

$$\frac{\partial^2 \ln q}{\partial \varphi^2} + \frac{\partial^2 \ln \rho}{\partial \varphi^2} + \frac{\partial^2 \ln \sin\theta}{\partial \varphi^2} + B\left(\frac{\partial \bar{e}_2}{\partial \varphi} \cdot \frac{\partial \bar{e}_1}{\partial \psi} - \frac{\partial \bar{e}_2}{\partial \psi} \cdot \frac{\partial \bar{e}_1}{\partial \varphi}\right) + A\left(\frac{\partial \bar{e}_3}{\partial \varphi} \cdot \frac{\partial \bar{e}_1}{\partial \eta} - \frac{\partial \bar{e}_3}{\partial \eta} \cdot \frac{\partial \bar{e}_1}{\partial \varphi}\right)$$

$$+ B^2\left(\frac{\partial \ln B}{\partial \psi} \frac{\partial \ln q}{\partial \psi} + \frac{\partial^2 \ln q}{\partial \psi^2}\right) + A^2\left(\frac{\partial \ln A}{\partial \eta} \frac{\partial \ln q}{\partial \eta} + \frac{\partial^2 \ln q}{\partial \eta^2}\right)$$

$$- \frac{\partial \ln B}{\partial \varphi}\left(\frac{\partial \ln q}{\partial \varphi} + \frac{\partial \ln B}{\partial \varphi}\right) - \frac{\partial \ln A}{\partial \varphi}\left(\frac{\partial \ln q}{\partial \varphi} + \frac{\partial \ln A}{\partial \varphi}\right) = 0 \qquad (17e)$$

Equation (17e) can be further simplified by noting (appendix C) that the fourth and fifth terms are related to the total curvatures K_η and K_ψ of the η and ψ stream surfaces, respectively, by

$$-\frac{K_\eta}{q^2} = B\left(\frac{\partial \bar{e}_2}{\partial \varphi} \cdot \frac{\partial \bar{e}_1}{\partial \psi} - \frac{\partial \bar{e}_2}{\partial \psi} \cdot \frac{\partial \bar{e}_1}{\partial \varphi}\right) \tag{17f}$$

$$-\frac{K_\psi}{q^2} = A\left(\frac{\partial \bar{e}_3}{\partial \varphi} \cdot \frac{\partial \bar{e}_1}{\partial \eta} - \frac{\partial \bar{e}_3}{\partial \eta} \cdot \frac{\partial \bar{e}_1}{\partial \varphi}\right) \tag{17g}$$

Thus, from equations (17e), (17f), and (17g),

$$\frac{\partial^2 \ln q}{\partial \varphi^2} + \frac{\partial^2 \ln \rho}{\partial \varphi^2} + \frac{\partial^2 \ln \sin \theta}{\partial \varphi^2} - \frac{K_\eta}{q^2} - \frac{K_\psi}{q^2}$$

$$+ B^2\left(\frac{\partial \ln B}{\partial \psi}\frac{\partial \ln q}{\partial \psi} + \frac{\partial^2 \ln q}{\partial \psi^2}\right) - \frac{\partial \ln B}{\partial \varphi}\left(\frac{\partial \ln q}{\partial \varphi} + \frac{\partial \ln B}{\partial \varphi}\right)$$

$$+ A^2\left(\frac{\partial \ln A}{\partial \eta}\frac{\partial \ln q}{\partial \eta} + \frac{\partial^2 \ln q}{\partial \eta^2}\right) - \frac{\partial \ln A}{\partial \varphi}\left(\frac{\partial \ln q}{\partial \varphi} + \frac{\partial \ln A}{\partial \varphi}\right) = 0 \tag{17h}$$

Equation (17h) is the governing, second-order, partial-differential equation for the distribution of $\ln q$ in transformed φ,ψ,η-space. This equation is also developed (appendix D) directly from separate considerations of the two-dimensional continuity and irrotationality flow conditions in η and ψ stream laminae; the results are then interrelated by the simple continuity equation (10d) for three-dimensional flow.

Incompressible flow. - For incompressible flow, the density ρ is 1.0. Thus the second term in the governing differential equation (17h) disappears, and the density no longer affects the values of A and B given by equations (10a) and (10b), respectively.

Plane two-dimensional flow. - For plane, two-dimensional flow,

$$K_\eta = 0$$

$$K_\psi = 0$$

$$\theta = 90^\circ$$

$$\frac{dm}{d\eta} = 1$$

$$\frac{dn}{d\psi} = \frac{1}{\rho q}$$

$$\frac{\partial}{\partial \eta} = 0$$

so that, from equations (10a) and (10b),

$$A = \rho \frac{dn}{d\psi} \sin \theta = \frac{1}{q}$$

$$B = \rho \frac{dm}{d\eta} \sin \theta = \rho$$

from which

$$\frac{\partial \ln A}{\partial \varphi}\left(\frac{\partial \ln q}{\partial \varphi} + \frac{\partial \ln A}{\partial \varphi}\right) = -\frac{\partial \ln q}{\partial \varphi}\left(\frac{\partial \ln q}{\partial \varphi} - \frac{\partial \ln q}{\partial \varphi}\right) = 0$$

Thus, for plane, two-dimensional flow, the governing differential equation (17h) reduces to

$$\frac{\partial^2 \ln q}{\partial \varphi^2} + \frac{\partial^2 \ln \rho}{\partial \varphi^2} + \rho^2\left(\frac{\partial \ln \rho}{\partial \psi}\frac{\partial \ln q}{\partial \psi} + \frac{\partial^2 \ln q}{\partial \psi^2}\right) - \frac{\partial \ln \rho}{\partial \varphi}\left(\frac{\partial \ln q}{\partial \varphi} + \frac{\partial \ln \rho}{\partial \varphi}\right) = 0 \quad (18a)$$

Equation (18a) is the governing differential equation (7) in reference 1.

For incompressible flow ($\rho = 1$), equation (18a) becomes

$$\frac{\partial^2 \ln q}{\partial \varphi^2} + \frac{\partial^2 \ln q}{\partial \psi^2} = 0 \quad (18b)$$

Axisymmetric two-dimensional flow. - For axisymmetric, two-dimensional flow,

$$\left.\begin{aligned} K_\eta &= 0 \\ \theta &= 90^\circ \end{aligned}\right\} \quad (19a)$$

(continued)

$$\left.\begin{aligned} \frac{dm}{d\eta} &= r \\ \frac{dn}{d\psi} &= \frac{1}{\rho r q} \\ \frac{\partial}{\partial \eta} &= 0 \end{aligned}\right\} \tag{19a}$$

and, except for $\partial \bar{e}_3/\partial\eta$,

where r is the radius from the axis. Thus, from equation (10a),

$$\left.\begin{aligned} A &= \rho \frac{dn}{d\psi} \sin\theta = \frac{1}{rq} \\ \frac{\partial \ln A}{\partial \varphi} &= -\left(\frac{\partial \ln q}{\partial \varphi} + \frac{\partial \ln r}{\partial \varphi}\right) \\ \frac{\partial^2 \ln A}{\partial \varphi^2} &= -\left(\frac{\partial^2 \ln q}{\partial \varphi^2} + \frac{\partial^2 \ln r}{\partial \varphi^2}\right) \end{aligned}\right\} \tag{19b}$$

and, from equation (10b),

$$\left.\begin{aligned} B &= \rho \frac{dm}{d\eta} \sin\theta = \rho r \\ \frac{\partial \ln B}{\partial \varphi} &= \frac{\partial \ln \rho}{\partial \varphi} + \frac{\partial \ln r}{\partial \varphi} \\ \frac{\partial \ln B}{\partial \psi} &= \frac{\partial \ln \rho}{\partial \psi} + \frac{\partial \ln r}{\partial \psi} \end{aligned}\right\} \tag{19c}$$

Also, from equations (C6) and (19b),

$$-\frac{K_\psi}{q^2} = \frac{\partial^2 \ln r}{\partial \varphi^2} + \frac{\partial \ln r}{\partial \varphi}\left(\frac{\partial \ln q}{\partial \varphi} + \frac{\partial \ln r}{\partial \varphi}\right) \tag{19d}$$

Thus, from equations (19a) to (19d), the governing differential equation (17h) reduces to

$$\frac{\partial^2 \ln q}{\partial \varphi^2} + \frac{\partial^2 \ln \rho}{\partial \varphi^2} + \frac{\partial^2 \ln r}{\partial \varphi^2} - \left(\frac{\partial \ln \rho}{\partial \varphi} + \frac{\partial \ln r}{\partial \varphi}\right)\left(\frac{\partial \ln q}{\partial \varphi} + \frac{\partial \ln \rho}{\partial \varphi} + \frac{\partial \ln r}{\partial \varphi}\right)$$

$$+ \rho^2 r^2 \left[\left(\frac{\partial \ln \rho}{\partial \psi} + \frac{\partial \ln r}{\partial \psi}\right)\frac{\partial \ln q}{\partial \psi} + \frac{\partial^2 \ln q}{\partial \psi^2}\right] = 0 \qquad (19e)$$

For axisymmetric, two-dimensional, compressible flow, equation (19e) is the governing differential equation for the distribution of $\ln q$ on the transformed φ, ψ-plane.

For incompressible flow ($\rho = 1$), equation (19e) reduces to

$$\frac{\partial^2 \ln q}{\partial \varphi^2} + \frac{\partial^2 \ln r}{\partial \varphi^2} - \frac{\partial \ln r}{\partial \varphi}\left(\frac{\partial \ln q}{\partial \varphi} + \frac{\partial \ln r}{\partial \varphi}\right) + r^2 \left(\frac{\partial \ln r}{\partial \psi}\frac{\partial \ln q}{\partial \psi} + \frac{\partial^2 \ln q}{\partial \psi^2}\right) = 0 \qquad (19f)$$

Equation (19f) is the governing differential equation (11) in reference 2.

Construction of Physical Flow Field

For prescribed distributions of velocity along the boundary streamlines, the objective of this design method is the construction of the physical flow field, particularly the shape of its boundary, in x, y, z-space. From every finite-difference solution of the governing differential equation (17h), in a series of iterative solutions, each with fixed distributions of A, B, ρ, and $\sin\theta$ throughout the flow field, the distribution of velocity, that is, of $\ln q$, is known in φ, ψ, η-space. From this distribution of velocity, the shape of the flow field in physical x, y, z-space can be determined by methods, developed in this section, using various equations introduced during the development of the governing equation (17h).

Outline of construction method. - After the governing equation (17h) has been solved for the distribution of $\ln q$ (by finite-difference techniques), the unit vectors $\bar{e}_1$, $\bar{e}_2$, and $\bar{e}_3$; the physical coordinate x, y, and z; the angle θ; and the parameters A and B can be determined as follows:

(1) Assume that $\bar{e}_1$, $\bar{e}_2$, $\bar{e}_3$, x, y, z, θ, A, and B are known for a given φ-surface. For example, this surface is initially the upstream boundary ($\varphi = 0.0$), where, as shown later, x, y, and z are known and with $\bar{q}$ equal to $\bar{e}_1$ ($q = q_U = 1.0$) and θ equal to 90°,

$$\left.\begin{aligned} \bar{e}_1 &= \bar{i} \\ \bar{e}_2 &= \bar{j} \\ \bar{e}_3 &= \bar{k} \\ A &= 1 \\ B &= 1 \end{aligned}\right\} \tag{20}$$

(2) The object then is to determine $\bar{e}_1$, $\bar{e}_2$, $\bar{e}_3$, x, y, z, θ, A, and B for the next downstream φ-surface.

(3) This object is achieved by the following procedure, which is described more fully in subsequent sections:

(a) From equations (7a), (13e), and (13f), determine the distribution of $\bar{e}_1$ on the next potential surface in x, y, z-space.

(b) From equations (7c), (13e) (with $\bar{e}_1 \cdot \bar{e}_2 = 0$), and (14c), determine the distribution of $\bar{e}_2$ on the next potential surface.

(c) From equations (7e), (13f) (with $\bar{e}_1 \cdot \bar{e}_3 = 0$), and (14d), determine the distribution of $\bar{e}_3$ on the next potential surface.

(d) Determine the distribution of θ on the next potential surface from equation (8c).

(e) Determine the distributions of x-, y-, and z-coordinates on the next potential surface by methods to be presented.

(f) Determine the distributions of A and B on the next potential surface from equations (10a) and (10b), respectively, in which ρ and $\sin\theta$ are known and where $dn/d\psi$ and $dm/d\eta$ follow directly from the distributions of x, y, and z obtained in step (e). (Alternative methods, which are discussed later, may be used for the determination of A and B.)

Unit vector $\bar{e}_1$. - From equation (7a),

$$\bar{e}_1 \cdot \bar{e}_1 = \cos^2\alpha_1 + \cos^2\beta_1 + \cos^2\gamma_1 = 1 \tag{21a}$$

$$\frac{\partial \bar{e}_1}{\partial \varphi} = \bar{i}\,\frac{\partial \cos\alpha_1}{\partial \varphi} + \bar{j}\,\frac{\partial \cos\beta_1}{\partial \varphi} + \bar{k}\,\frac{\partial \cos\gamma_1}{\partial \varphi} \tag{21b}$$

where, from equations (13e), (13f), and (21a),

$$\frac{\partial \cos \alpha_1}{\partial \varphi} = -\frac{\cos \beta_1}{\cos \alpha_1} \frac{\partial \cos \beta_1}{\partial \varphi} - \frac{\cos \gamma_1}{\cos \alpha_1} \frac{\partial \cos \gamma_1}{\partial \varphi} \tag{21c}$$

$$\frac{\partial \cos \beta_1}{\partial \varphi} = \frac{C_2^* P_3 \cos \alpha_1 - C_1^* P_4 \cos \alpha_1}{P_1 P_4 - P_2 P_3} \tag{21d}$$

$$\frac{\partial \cos \gamma_1}{\partial \varphi} = \frac{C_2^* P_1 \cos \alpha_1 - C_1^* P_2 \cos \alpha_1}{P_2 P_3 - P_1 P_4} \tag{21e}$$

in which

$$\left.\begin{aligned} C_1^* &= B \frac{\partial \ln q}{\partial \psi} \\ C_2^* &= A \frac{\partial \ln q}{\partial \eta} \end{aligned}\right\} \tag{21f}$$

$$\left.\begin{aligned} P_1 &= \cos \alpha_2 \cos \beta_1 - \cos \alpha_1 \cos \beta_2 \\ P_2 &= \cos \alpha_3 \cos \beta_1 - \cos \alpha_1 \cos \beta_3 \\ P_3 &= \cos \alpha_2 \cos \gamma_1 - \cos \alpha_1 \cos \gamma_2 \\ P_4 &= \cos \alpha_3 \cos \gamma_1 - \cos \alpha_1 \cos \gamma_3 \end{aligned}\right\} \tag{21g}$$

Integration of equations (21c), (21d), and (21e) determines the distributions of $\cos \alpha_1$, $\cos \beta_1$, and $\cos \gamma_1$, respectively, and, thereby, from equation (7a), the distribution of $\bar{e}_1$ on the next potential surface.

Unit vector $\bar{e}_2$. - From equation (7c),

$$\bar{e}_2 \cdot \bar{e}_2 = \cos^2 \alpha_2 + \cos^2 \beta_2 + \cos^2 \gamma_2 = 1 \tag{22a}$$

$$\frac{\partial \bar{e}_2}{\partial \varphi} = \bar{i} \frac{\partial \cos \alpha_2}{\partial \varphi} + \bar{j} \frac{\partial \cos \beta_2}{\partial \varphi} + \bar{k} \frac{\partial \cos \gamma_2}{\partial \varphi} \tag{22b}$$

where, from equations (13e) (with $\bar{e}_1 \cdot \bar{e}_2 = 0$), (14c), and (22a),

$$\frac{\partial \cos \alpha_2}{\partial \varphi} = -\frac{\cos \beta_2}{\cos \alpha_2} \frac{\partial \cos \beta_2}{\partial \varphi} - \frac{\cos \gamma_2}{\cos \alpha_2} \frac{\partial \cos \gamma_2}{\partial \varphi} \tag{22c}$$

$$\frac{\partial \cos \beta_2}{\partial \varphi} = \frac{C_1^* P_7 \cos \alpha_2 + C_3^* P_8 \cos \alpha_2}{P_6 P_7 - P_5 P_8} \tag{22d}$$

$$\frac{\partial \cos \gamma_2}{\partial \varphi} = \frac{C_1^* P_5 \cos \alpha_2 + C_3^* P_6 \cos \alpha_2}{P_5 P_8 - P_6 P_7} \tag{22e}$$

in which

$$C_3^* = B\left[(\cos \alpha_3 - \cos \alpha_2 \cos \theta) \frac{\partial \cos \alpha_1}{\partial \psi} + (\cos \beta_3 - \cos \beta_2 \cos \theta) \frac{\partial \cos \beta_1}{\partial \psi} + (\cos \gamma_3 - \cos \gamma_2 \cos \theta) \frac{\partial \cos \gamma_1}{\partial \psi}\right] \tag{22f}$$

$$\left.\begin{aligned} P_5 &= \cos \alpha_3 \cos \beta_2 - \cos \alpha_2 \cos \beta_3 \\ P_6 = -P_1 &= \cos \alpha_1 \cos \beta_2 - \cos \alpha_2 \cos \beta_1 \\ P_7 &= \cos \alpha_3 \cos \gamma_2 - \cos \alpha_2 \cos \gamma_3 \\ P_8 = -P_3 &= \cos \alpha_1 \cos \gamma_2 - \cos \alpha_2 \cos \gamma_1 \end{aligned}\right\} \tag{22g}$$

Integration of equations (22c), (22d), and (22e) determines the distributions of $\cos \alpha_2$, $\cos \beta_2$, and $\cos \gamma_2$, respectively, and, thereby, from equation (7c), the distribution of $\bar{e}_2$ on the next potential surface.

Unit vector $\bar{e}_3$. - From equation (7e),

$$\bar{e}_3 \cdot \bar{e}_3 = \cos^2 \alpha_3 + \cos^2 \beta_3 + \cos^2 \gamma_3 = 1 \tag{23a}$$

$$\frac{\partial \bar{e}_3}{\partial \varphi} = \bar{i} \frac{\partial \cos \alpha_3}{\partial \varphi} + \bar{j} \frac{\partial \cos \beta_3}{\partial \varphi} + \bar{k} \frac{\partial \cos \gamma_3}{\partial \varphi} \tag{23b}$$

where, from equations (13f) (with $\bar{e}_1 \cdot \bar{e}_3 = 0$), (14d), and (23a),

$$\frac{\partial \cos \alpha_3}{\partial \varphi} = -\frac{\cos \beta_3}{\cos \alpha_3} \frac{\partial \cos \beta_3}{\partial \varphi} - \frac{\cos \gamma_3}{\cos \alpha_3} \frac{\partial \cos \gamma_3}{\partial \varphi} \tag{23c}$$

$$\frac{\partial \cos \beta_3}{\partial \varphi} = \frac{C_2^* P_9 \cos \alpha_3 + C_4^* P_{10} \cos \alpha_3}{P_{12} P_9 - P_{11} P_{10}} \tag{23d}$$

$$\frac{\partial \cos \gamma_3}{\partial \varphi} = \frac{C_2^* P_{11} \cos \alpha_3 + C_4^* P_{12} \cos \alpha_3}{P_{11} P_{10} - P_{12} P_9} \tag{23e}$$

in which

$$C_4^* = A \left[(\cos \alpha_2 - \cos \alpha_3 \cos \theta) \frac{\partial \cos \alpha_1}{\partial \eta} + (\cos \beta_2 - \cos \beta_3 \cos \theta) \frac{\partial \cos \beta_1}{\partial \eta} + (\cos \gamma_2 - \cos \gamma_3 \cos \theta) \frac{\partial \cos \gamma_1}{\partial \eta} \right] \tag{23f}$$

$$\left.\begin{aligned} P_9 &= -P_7 = \cos \alpha_2 \cos \gamma_3 - \cos \alpha_3 \cos \gamma_2 \\ P_{10} &= -P_4 = \cos \alpha_1 \cos \gamma_3 - \cos \alpha_3 \cos \gamma_1 \\ P_{11} &= -P_5 = \cos \alpha_2 \cos \beta_3 - \cos \alpha_3 \cos \beta_2 \\ P_{12} &= -P_2 = \cos \alpha_1 \cos \beta_3 - \cos \alpha_3 \cos \beta_1 \end{aligned}\right\} \tag{23g}$$

Integration of equations (23c), (23d), and (23e) determines the distributions of $\cos \alpha_3$, $\cos \beta_3$, and $\cos \gamma_3$, respectively, and, thereby, from equation (7e), the distribution of $\bar{e}_3$ on the next potential surface.

Parameter A. - The parameter A comes directly from its definition, equation (10a):

$$A = \rho \frac{\Delta n}{\Delta \psi} \sin \theta \tag{24}$$

where Δn follows directly from known values of Δx, Δy, and Δz (corresponding to $\Delta\psi$ and obtained as described in a later section) on the next potential surface. Equation (24) determines the distribution of parameter A on the next potential surface.

Parameter B. - The parameter B comes directly from its definition, equation (10b):

$$B = \rho \frac{\Delta m}{\Delta \eta} \sin \theta \tag{25}$$

where Δm follows directly from known values of Δx, Δy, and Δz (corresponding to $\Delta\eta$ and obtained as described in the next section) on the next potential surface. Equation (25) determines the distribution of parameter B on the next potential surface.

Although in theory the values of A and B are determined by equations (24) and (25), respectively, in practice, the values may be better determined, during the iteration process, by equation (10d) and the ratio of equations (24) and (25) or by equation (10d) and the difference of equations (16c) and (16d), which difference gives

$$\frac{\partial\left(\frac{A}{B}\right)}{\partial\varphi} = \frac{A}{B}\left(B\bar{e}_2 \cdot \frac{\partial \bar{e}_1}{\partial\psi} - A\bar{e}_3 \cdot \frac{\partial \bar{e}_1}{\partial\eta}\right)$$

Coordinates of flow field in x, y, z-space. - The x, y, z-coordinates corresponding to points in the flow field of φ, ψ, η-space, which coordinates establish the shape of the flow field in physical x, y, z-space, are obtained from the direction cosines. Thus, from equation (7b), along a φ-curve of constant ψ and η,

$$\frac{\partial x}{\partial s} = \cos \alpha_1$$

$$\frac{\partial x}{\partial \varphi}\frac{d\varphi}{ds} = \cos \alpha_1$$

so that, from equation (5f),

$$x = x_U + \int_0^{\varphi} \left(\frac{\cos \alpha_1}{q}\right) d\varphi \tag{26a}$$

Likewise

$$\frac{\partial y}{\partial s} = \frac{\partial y}{\partial \varphi}\frac{d\varphi}{ds} = \frac{\partial y}{\partial \varphi} q = \cos \beta_1$$

so that

$$y = y_U + \int_0^{\varphi} \left(\frac{\cos \beta_1}{q} \right) d\varphi \tag{26b}$$

And likewise

$$\frac{\partial z}{\partial s} = \frac{\partial z}{\partial \varphi} \frac{d\varphi}{ds} = \frac{\partial z}{\partial \varphi} q = \cos \gamma_1$$

so that

$$z = z_U + \int_0^{\varphi} \left(\frac{\cos \gamma_1}{q} \right) d\varphi \tag{26c}$$

Equations (26a), (26b), and (26c), which are integrals along streamlines of constant ψ and η, are sufficient to determine the physical shape of the flow field in x, y, z-space. In particular, for streamlines along the boundary, these equations determine the shape of the boundary.

In addition, along ψ- and η-curves on any potential surface of constant φ, the x, y, z-coordinates can be determined by other, redundant integrals. Thus, along a ψ-curve,

$$\frac{\partial x}{\partial n} = \cos \alpha_2$$

$$\frac{\partial x}{\partial \psi} \frac{d\psi}{dn} = \cos \alpha_2$$

so that, from equation (10e),

$$x = x_x + \int_{\psi_x}^{\psi} \left(\frac{\cos \alpha_2}{qB} \right) d\psi \tag{26d}$$

where the subscript x refers to conditions at the lower bound of the integral. Likewise

$$\frac{\partial y}{\partial n} = \frac{\partial y}{\partial \psi} \frac{d\psi}{dn} = \frac{\partial y}{\partial \psi} qB = \cos \beta_2$$

so that

$$y = y_x = \int_{\psi_x}^{\psi} \left(\frac{\cos \beta_2}{qB} \right) d\psi \tag{26e}$$

And likewise

$$\frac{\partial z}{\partial n} = \frac{\partial z}{\partial \psi} \frac{d\psi}{dn} = \frac{\partial z}{\partial \psi} qB = \cos \gamma_2$$

so that

$$z = z_x + \int_{\psi_x}^{\psi} \left(\frac{\cos \gamma_2}{qB} \right) d\psi \tag{26f}$$

Equations (26d), (26e), and (26f) determine the x, y, z-coordinates on any potential surface of constant φ from integrals along lines of constant η on that surface in φ, ψ, η-space.

Also, along an η-curve on any potential surface,

$$\frac{\partial x}{\partial m} = \cos \alpha_3$$

$$\frac{\partial x}{\partial \eta} \frac{d\eta}{dm} = \cos \alpha_3$$

so that, from equation (10g),

$$x = x_x + \int_{\eta_x}^{\eta} \left(\frac{\cos \alpha_3}{qA} \right) d\eta \tag{26g}$$

Likewise

$$\frac{\partial y}{\partial m} = \frac{\partial y}{\partial \eta} \frac{d\eta}{dm} = \frac{\partial y}{\partial \eta} qA = \cos \beta_3$$

so that

$$y = y_x + \int_{\eta_x}^{\eta} \left(\frac{\cos \beta_3}{qA} \right) d\eta \tag{26h}$$

And likewise

$$\frac{\partial z}{\partial m} = \frac{\partial z}{\partial \eta} \frac{d\eta}{dm} = \frac{\partial z}{\partial \eta} qA = \cos \gamma_3$$

so that

$$z = z_x + \int_{\eta_x}^{\eta} \left(\frac{\cos \gamma_3}{qA} \right) d\eta \tag{26i}$$

Equations (26g), (26h), and (26i) determine the x, y, z-coordinates on any potential surface of constant φ from integrals along lines of constant ψ on that surface in φ, ψ, η-space.

The shape of the flow field in x, y, z-space, including the boundary shape, is given by the x, y, z-coordinates determined from equations (26a) to (26i).

DESIGN PROCEDURE

The design procedure, using equations developed in the section THEORY OF DESIGN METHOD, is outlined in this section. After general aspects are considered, special problems associated with internal flow fields and external flow fields are discussed, and a brief step-by-step numerical procedure is presented.

General Considerations

General aspects of the design procedure that are independent of the internal or external nature of the flow field are considered here. These aspects include (1) the flow field configuration in φ, ψ, η-space, (2) finite-difference grid points of the flow field in φ, ψ, η-space, (3) the finite difference form of the governing differential equation, (4) the specified velocity distribution on boundaries of the flow field, (5) stagnation points, and (6) planes of symmetry.

Flow field configuration in φ, ψ, η-space. - Because the lateral boundary of the flow field in x, y, z- and in φ, ψ, η-space always contains the same streamlines of constant ψ and η, the shape of every potential plane in φ, ψ, η-space is the same, and because the

upstream and downstream boundaries are surfaces of constant φ, the flow field configuration in transformed φ, ψ, η-space is a right cylinder, as shown in figure 9, or a rectangular parallelepiped.

The shape of the flow field on the potential planes in φ, ψ, η-space depends on the specified shape of the upstream boundary area in physical x, y, z-space and on the specified arrangement of the fluid lines on that area (lines of constant ψ and η, see the section Stream functions $\psi(x, y, z)$ and $\eta(x, y, z)$). Because this arrangement is somewhat arbitrary (provided only that equation (6d) is satisfied), it is generally convenient to have the fluid lines of constant ψ intersect the fluid lines of constant η at right angles. Thus the angle θ is 90° at the upstream boundary. As a result, from the continuity equation (9d), at the upstream boundary, where ρ and q are 1.0,

$$d\psi \, d\eta = dn \, dm \tag{27a}$$

In addition, if a Cartesian grid of fluid lines is used (as opposed to a polar grid, for which θ is also 90°), then, because the flow is uniform everywhere on the upstream boundary,

$$\frac{d\psi}{dn} = \frac{d\eta}{dm} \tag{27b}$$

From equations (27a) and (27b), it follows that

$$\left.\begin{aligned} d\psi &= dn \\ d\eta &= dm \end{aligned}\right\} \tag{27c}$$

Thus the shape of the upstream boundary in φ, ψ, η-space is the same as the specified shape of the upstream boundary in x, y, z-space.

If a polar grid of fluid lines, instead of the Cartesian grid, is used at the upstream boundary in x, y, z-space, the shape of the upstream boundary in φ, ψ, η-space is different. This case is considered later in the report.

Grid points of flow field in φ, ψ, η-space. - The finite-difference solution of the governing differential equation (17h) requires a three-dimensional grid of finitely spaced points in transformed φ, ψ, η-space; at these grid points, ln q and other properties of the flow field are determined. This grid is formed by the intersections of planes of constant φ, ψ, and η spaced a_1, a_2, and a_3 distances apart, respectively, as shown in figure 9. These distances, although constant between any two adjacent planes, need not be the same for all planes. The grid also includes the intersections of ψ and η stream planes with the boundary of the flow field on potential planes of constant φ (fig. 9). It is at these boundary grid points that the velocity distribution is

specified. Obviously the a_2 or a_3 spacing of a boundary grid point from its adjacent, internal grid point on the potential plane is not, in general, uniform.

From the above discussion, for every internal grid point of the flow field in φ,ψ,η-space, there exists a three-dimensional, finite-difference star (fig. 10) consisting of the grid point itself (marked 0) and its six adjacent grid points (marked 1 to 6). In this star, the lengths $a_1, a_2, \ldots, a_6$ are not, in general, equal. It is this star that is used in the finite-difference solution of equation (17h). The star is in its simplest form, and, in some applications, greater complexity, involving more grid points, may be required.

Corresponding to the grid in φ,ψ,η-space is a grid in x, y, z-space. This grid in x, y, z-space constitutes the solution and is given by x, y, z-coordinates determined, after the solution of equation (17h), by equations (26a) to (26i) at the grid points in φ,ψ-η-space.

Finite-difference form of governing differential equation. - In the governing differential equation (17h), first and second partial derivatives of ln q with respect to φ, ψ, and η can be expressed in finite-difference form by assuming that, in the immediate neighborhood of the central grid point 0 in the finite-difference star of figure 10, the distribution of ln q can be represented by a Taylor series expansion, which, for the three-point systems of this star, is equivalent to a parabolic distribution of ln q through the three grid points in each of the three directions φ, ψ, and η. For such distributions, the first derivative at the central point 0 is given by

$$\left(\frac{\partial Q}{\partial x_i}\right)_0 = \frac{Q_+ - Q_0}{\frac{\Delta x_+}{\Delta x_-}(\Delta x_+ + \Delta x_-)} - \frac{Q_- - Q_0}{\frac{\Delta x_-}{\Delta x_+}(\Delta x_+ + \Delta x_-)} \tag{28a}$$

where Q is ln q, x_i is distance in the φ-, ψ-, or η-direction, the subscripts + and - refer to values in the positive or negative direction from the central grid point 0, and Δx is the distance between adjacent grid points in φ,ψ,η-space. The second partial derivative is likewise given by

$$\left(\frac{\partial^2 Q}{\partial x_i^2}\right)_0 = \frac{2(Q_+ - Q_0)}{\Delta x_+(\Delta x_+ + \Delta x_-)} + \frac{2(Q_- - Q_0)}{\Delta x_-(\Delta x_+ + \Delta x_-)} \tag{28b}$$

If the distances between adjacent grid points in a given direction are equal,

$$\Delta x_+ = \Delta x_- = \Delta x$$

and equations (28a) and (28b) reduce to

$$\left(\frac{\partial Q}{\partial x_i}\right)_0 = \frac{Q_+ - Q_-}{2\,\Delta x} \tag{28c}$$

$$\left(\frac{\partial^2 Q}{\partial x_i^2}\right)_0 = \frac{Q_+ + Q_- - 2Q_0}{(\Delta x)^2} \tag{28d}$$

Introducing the finite-difference equations (28a) and (28b) into the governing differential equation (17h) and using the nomenclature from the finite-difference star in figure 10 result in

$$C_C + C_1 Q_1 + C_2 Q_2 + C_3 Q_3 + C_4 Q_4 + C_5 Q_5 + C_6 Q_6 - C_0 Q_0 = \mathcal{R} \tag{28e}$$

where

$$\left.\begin{aligned}
C_C &= \frac{\partial^2 \ln \rho}{\partial \varphi^2} + \frac{\partial^2 \ln \sin\theta}{\partial \varphi^2} - \left(\frac{\partial \ln B}{\partial \varphi}\right)^2 - \left(\frac{\partial \ln A}{\partial \varphi}\right)^2 - \frac{K_\eta + K_\psi}{\exp(2Q_0)} \\
C_1 &= \frac{a_4}{a_1(a_1 + a_4)}\left(\frac{2}{a_4} - \frac{\partial \ln B}{\partial \varphi} - \frac{\partial \ln A}{\partial \varphi}\right) \\
C_2 &= \frac{a_5 B^2}{a_2(a_2 + a_5)}\left(\frac{2}{a_5} + \frac{\partial \ln B}{\partial \psi}\right) \\
C_3 &= \frac{a_6 A^2}{a_3(a_3 + a_6)}\left(\frac{2}{a_6} + \frac{\partial \ln A}{\partial \eta}\right) \\
C_4 &= \frac{a_1}{a_4(a_1 + a_4)}\left(\frac{2}{a_1} + \frac{\partial \ln B}{\partial \varphi} + \frac{\partial \ln A}{\partial \varphi}\right) \\
C_5 &= \frac{a_2 B^2}{a_5(a_2 + a_5)}\left(\frac{2}{a_2} - \frac{\partial \ln B}{\partial \psi}\right) \\
C_6 &= \frac{a_3 A^2}{a_6(a_3 + a_6)}\left(\frac{2}{a_3} - \frac{\partial \ln A}{\partial \eta}\right) \\
C_0 &= \frac{2}{a_1 a_4} + B^2\left(\frac{\partial \ln B}{\partial \psi}\frac{a_5 - a_2}{a_2 a_5} + \frac{2}{a_2 a_5}\right) + A^2\left(\frac{\partial \ln A}{\partial \eta}\frac{a_6 - a_3}{a_3 a_6} + \frac{2}{a_3 a_6}\right) - \left(\frac{\partial \ln B}{\partial \varphi} + \frac{\partial \ln A}{\partial \varphi}\right)\left(\frac{a_4 - a_1}{a_1 a_4}\right)
\end{aligned}\right\} \tag{28f}$$

and $\mathcal{R}$ is the residual error, which measures the degree to which the values of Q at the grid points of the finite-difference star in figure 10 satisfy the governing differential equation. The value of $\mathcal{R}$ is reduced, or eliminated, at each interior point of the three-dimensional grid in φ, ψ, η-space by iteratively changing the values of Q_0 while maintaining constant values for the coefficients given by equation (28f). After the residuals at every interior grid point have been reduced to sufficiently low values, new values for the coefficients are computed from equations (28f), and the iterative process is repeated. This procedure is continued until the values of the maximum residuals have converged within the derived accuracy; at which point, the governing differential equation (17h) has been solved for the specified distribution of Q (i.e., ln q) on the boundary of the flow field in φ, ψ, η-space.

Specified velocity distribution on boundary of flow field in φ, ψ, η-space. - As described in the section Preliminary Considerations, the specified distribution of velocity q as a function of path length s along streamlines on the laterial boundary of the flow field in x, y, z-space translates directly into the distribution of q as a function of velocity potential φ along streamlines on the lateral boundary of the flow field in φ, ψ, η-space. This direct relation results from equation (5f). In this section, therefore, considerations are limited to the velocity distribution as a function of φ on the boundary of the flow field in φ, ψ, η-space.

For proper use of the governing differential equation (17h), the upstream boundary ($\varphi = 0$) and the downstream boundary ($\varphi = \varphi_D$) should be sufficiently far upstream and downstream, respectively, from the region of the lateral boundary in which velocity changes are specified that the velocity is constant, as specified, not only on both the upstream boundary (where $q = 1.0$) and the downstream boundary (where $q = q_D$), but also over substantial regions of the lateral boundary adjacent to the end boundaries.

In the region of the lateral boundary where velocity changes are specified, these changes should be at least piecewise continuous, both in the direction of φ along the streamlines and in the direction tangent to the boundary and normal to the streamlines. To assure adequate smoothness in the variation of prescribed velocity on the laterial boundary, specify the velocity q as a function of φ and as a function of the parameter p_U, where p_U is path length along the prescribed perimeter of the upstream flow area. Thus, on the lateral boundary,

$$q = q(\varphi, p_U) \tag{29a}$$

from which, because

$$\psi = \psi(p_U) \tag{29b}$$

$$\eta = \eta(p_U) \tag{29c}$$

it follows that

$$q = q(\varphi, \psi, \eta) \tag{29d}$$

Stagnation points. - Stagnation points, at which the velocity q is zero so that ln q becomes negative infinity, are singularities that occur on the boundaries of all bodies in external flow fields and, for internal flow fields, at the junction of branched ducts or on the nose and tail surfaces of centerbodies within ducts. The mathematical problems associated with these singularities are not treated in the present report. Instead low but reasonably positive velocities can be specified on the boundary in regions that would otherwise include a stagnation point. As a result, these regions of the boundary are cusped in physical x, y, z-space.

Planes of symmetry. - Planes of symmetry, for which the flow fields on each side are mirror images, can occur in both internal and external flow fields. These planes of symmetry are either parallel to or normal to the velocity vectors on the plane. Such planes can be treated as boundaries of the flow field in both φ, ψ, η- and x, y, z-space. On these boundaries of planar symmetry, the velocities are not specified, but instead the derivative of the velocity normal to the boundary is zero.

Internal Flow Fields

Internal flow fields are ducted flow fields in physical x, y, z-space. Examples are simple ducts, branched ducts, annular ducts, and ducts with centerbodies, including the nose and/or tail region. The three-dimensionality of these ducts implies that they are unsymmetrical, although the ducts can have planar symmetry (q.v.).

Upstream boundary. - The upstream boundary is a flat surface of constant velocity potential ($\varphi_U = 0.0$) in both x, y, z- and φ, ψ, η-space. The orientation of this boundary in x, y, z-space is arbitrary, but in this report, it is taken as the y, z-plane of constant x equal to 0.0, as shown in figure 11.

The shape of the upstream boundary in x, y, z-space is an arbitrary input that is specified by

$$y_U = y_U(p_U) \tag{30a}$$

$$z_U = z_U(p_U) \tag{30b}$$

where p_U is path length along the perimeter starting from the point marked on the positive y-axis in figure 11. The area of the upstream boundary, which area is equal to 1.0 (see the section Nondimensional forms), is then given by

$$1.0 = \frac{1}{2} \oint (y_U \, dz_U - z_U \, dy_U)$$

$$= \frac{1}{2} \oint \left[y_U \left(\frac{dz}{dp} \right)_U - z_U \left(\frac{dy}{dp} \right)_U \right] dp_U \tag{30c}$$

If the upstream boundary includes an inner perimeter, such as would be the case for an annular duct, the line integral includes the inner perimeter, which is connected to the outer perimeter by a line cut, as shown in sketch (a).

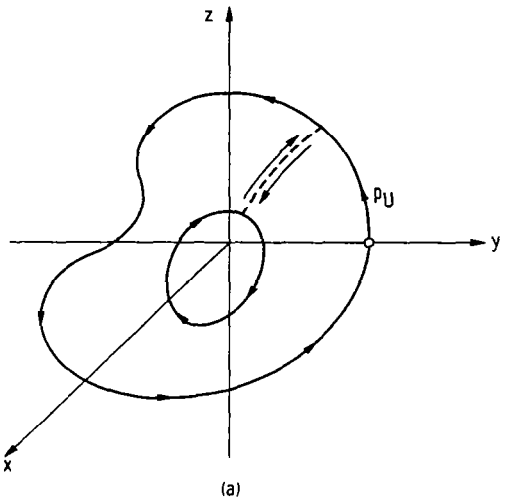

(a)

The intersections of the two sets of stream surfaces, $\psi(x, y, z)$ and $\eta(x, y, z)$, with the upstream boundary $\varphi(0, y, z) = 0$ in x, y, z-space are two sets of fluid lines that can be viewed as generating the stream surfaces as they move downstream with the flow. The specified (input) arrangement of these sets of fluid lines, that is, sets of constant $\psi(0, y_U, z_U)$ and sets of constant $\eta(0, y_U, z_U)$, on the upstream boundary is somewhat arbitrary, provided only that equation (6d) is satisfied, in which case the local angle θ_U with which the line of one set intersects that of the other is everywhere greater than zero and less than 180°. However, as observed previously, the arrangement of these fluid lines, together with the shape of the upstream boundary, both of which are input by the designer, dictates the shape of the flow field in φ, ψ, η-space. It is, therefore, convenient to arrange the fluid lines so that θ_U is everywhere equal to 90° on the upstream boundary. In particular, if the fluid lines are arranged so that

$$\left.\begin{aligned}\psi &= Cy_U \\ \eta &= Cz_U\end{aligned}\right\} \tag{30d}$$

where the constant C is the same for both equations, then from the continuity equation (9d),

$$\rho_U q_U \sin\theta_U = \left(\frac{d\psi}{dy}\,\frac{d\eta}{dz}\right)_U$$

or, because $\rho_U = 1.0$, $q_U = 1.0$, and $\theta_U = 90^o$,

$$C = 1.0$$

from which equations (30d) become

$$\left.\begin{aligned}\psi &= y_U \\ \eta &= z_U\end{aligned}\right\} \tag{30e}$$

Equation (30e) is similar to equation (27c).

Thus, in summary, the desired shape of the upstream boundary in x, y, z-space is specified, by the designer, on the y_U, z_U-plane, by

$$y_U = y_U(p_U) \tag{30a}$$

$$z_U = z_U(p_U) \tag{30b}$$

with fluid lines arranged on the upstream boundary so that

$$\left.\begin{aligned}\psi &= y_U \\ \eta &= z_U\end{aligned}\right\} \tag{30e}$$

where the nondimensional values of y_U and z_U are such that the upstream area A_U is 1.0. (In practice, the upstream shape is first specified in dimensional units from which the dimensional value of the upstream area is determined; the nondimensional coordinates, for which the upstream area is 1.0, are then obtained from equations (4a).)

For the previously specified arrangement of fluid lines, the arbitrary shape of the upstream boundary with a grid of ψ and η fluid lines is that shown in figure 11. It is noted that the $\Delta\psi$ grid spacing need not equal the $\Delta\eta$ spacing, and particularly, in this general case, the spacing for grid points adjacent to the boundary is variable. Because $\psi = y_U$ and $\eta = z_U$, the grid spacing and the shape of the upstream boundary are unchanged by the transformation from x, y, z-space to φ, ψ, η-space; in addition, this shape and grid remain unchanged with φ in φ, ψ, η-space. Of course, for upstream boundaries that are square or rectangular, the rectangular grid in figure 11 is ideal, because the grid spacing adjacent to the boundary need not be variable. (In this case, the grid points at the four corners of the boundary do not appear in the finite-difference star (fig. 10). Thus, in effect, these upstream boundaries may or may not have rounded corners with radii equal to or less than the Δy_U or Δz_U grid spacings, whichever is smaller.)

For circular upstream boundaries in x, y, z-space, including circular annuli and sectors of circular annuli, a circumferential and radial arrangement of the ψ and η fluid lines, respectively, is more convenient. For this arrangement, θ_U is again 90^o, and

$$\left.\begin{aligned} dn_U &= dr_U \\ dm_U &= r_U \, d\theta'_U \end{aligned}\right\} \tag{30f}$$

where

$$\left.\begin{aligned} r_U &= \sqrt{y_U^2 + z_U^2} \\ \theta'_U &= \tan^{-1} \frac{z_U}{y_U} \end{aligned}\right\} \tag{30g}$$

From equation (30c), with

$$\left.\begin{aligned} y_U &= r_U \cos \theta'_U \\ z_U &= r_U \sin \theta'_U \end{aligned}\right\} \tag{30h}$$

the nondimensional area A_U of the upstream boundary becomes

$$A_U = 1.0 = \frac{1}{2} \oint r_U^2 \, d\theta'_U \tag{30i}$$

or, for the special case of constant values of r_U with varying θ'_U,

$$1.0 = \frac{\Delta\theta'_U}{2} \left(r^2_{U,\max} - r^2_{U,\min} \right) \tag{30j}$$

where $r_{U,\max}$ and $r_{U,\min}$ are the outer and inner radii, respectively, and $\Delta\theta'_U$ is the included angle.

If, by definition, for this special case of constant r_U with varying θ'_U,

$$\eta = \frac{\theta'_U}{\Delta\theta'_U} \tag{30k}$$

so that the full range of η values goes from 0.0 to 1.0, then, from equations (30f) and from the continuity equation (9d),

$$\rho_U q_U \sin \theta_U = \frac{1}{r_U} \left(\frac{d\psi}{dr} \right)_U \left(\frac{d\eta}{d\theta'} \right)_U$$

or, because $\rho_U = 1.0$, $q_U = 1.0$, and θ_U is 90°,

$$d\psi = \Delta\theta'_U \, r_U \, dr_U$$

from which

$$\int_0^{\psi} d\psi = \Delta\theta'_U \int_{r_{U,\min}}^{r_U} r_U \, dr_U$$

or

$$\psi = \frac{\Delta\theta'_U}{2} \left(r^2_U - r^2_{U,\min} \right) \tag{30l}$$

From equation (30l), with r_U equal to $r_{U,\max}$,

$$\psi_{\max} = \frac{\Delta\theta'_U}{2} \left(r^2_{U,\max} - r^2_{U,\min} \right)$$

or, from equation (30j),

$$\psi_{max} = 1.0$$

so that the full range of ψ values goes from 0.0 to 1.0, as is the case for the η values.

For the previously specified arrangement of fluid lines, the shape of the upstream boundary is that shown in figure 12, in which the scale of the y_U, z_U-coordinates is such that the upstream boundary area A_U is 1.0. The fluid lines of constant ψ are here spaced, according to equation (30l), to give equal increments of ψ. However, as is the case for rectangular Cartesian grids, the $\Delta\psi$ and $\Delta\eta$ grid spacings need not be equal, except of course, between adjacent stream surfaces. In any event, for upstream boundaries with combinations of straight-radial and circular-arc contours, the grid spacing for points adjacent to the contour can be conveniently constant. Also, as for the rectangular Cartesian grid (q.v.), because the grid points at the four corners of the boundary do not appear in the finite-difference star (fig. 10), the upstream flow area can have, in effect, rounded corners, unless $\Delta\theta'_U$ equals 360^o. However, unlike the Cartesian grid arrangement, for which the shape of the upstream boundary remains unchanged by the transformation, for this polar grid arrangement of fluid lines, the shape of the upstream boundary changes from one with circular features in x, y, z-space to one with a rectangular shape in φ, ψ, η-space.

Because, for potential flow, the solution is reversible, in some cases the shape of the upstream boundary, which shape is arbitrarily specified, can in fact be the desired shape of the downstream boundary, in which case the so-called downstream boundary becomes the upstream boundary, and its shape is not specified, but depends on the specified velocity distributions on the boundary of the entire flow field. This feature of reversible flow means that, for example, either the upstream or the downstream shape of flow area, but not both, can be specified to have constant radii at hub and/or shroud, so as to match the axisymmetric surfaces of turbomachine annuli.

In figure 12, if $r_{U,min}$ is zero, a singularity exists at the origin, where η takes on its full range of values. However, in φ, ψ, η-space, where the design problem is solved, the singularity disappears with the η values equally spaced along the boundary line for ψ equal to zero at constant φ. (Along this boundary line, the velocity is then constant.)

This polar arrangement of fluid lines on the upstream boundary, with its associated singularity, becomes essential when the duct includes a centerbody that starts downstream from the duct inlet. For this case, the stagnation streamline at the upstream boundary is located at the origin ($r_{U,min} = 0.0$, in fig. 12), where ψ is 0.0 and η has its full range of values. Downstream from the stagnation point (q.v.) on the centerbody, the value of ψ is then everywhere 0.0, and a grid of η and φ lines covers the

centerbody surface. This situation is shown in figure 13 for the simple case of incompressible, potential flow around a sphere.

Of course, it is not necessary that the upstream boundary contour conform to the fluid lines of constant ψ and η in figure 12. In fact, an arbitrary shape, such as that in figure 11, could equally well be treated by this polar grid arrangement, in which case, the integrand r_U^2 of equation (30i) would vary with θ'_U along the line integral.

Specified velocity distribution on boundary. - The specified velocity distributions on the upstream and downstream boundaries are normally uniform, unless either or both of these surfaces are planes of symmetry (q.v.), in which case, the velocity is not specified, and instead, the boundary condition becomes $\partial \ln q/\partial\varphi = 0.0$. For those cases in which the velocity is uniform, the nondimensional upstream velocity q_U is 1.0, and the downstream velocity q_D can have any value, provided it is not supersonic.

Along the duct wall, the velocity distribution is prescribed as discussed previously in the section General Considerations. In addition, for the polar grid arrangement of fluid lines on the upstream boundary, if $\Delta\theta'_U$ (fig. 12) is 360^o, then, on the two surfaces of constant η equal to 0.0 and 1.0, the boundary condition is that the velocity (which is not input) is the same at corresponding φ,ψ-points.

For planar symmetry (q.v.) parallel to the direction of flow, it is necessary to design only the part of the duct that lies between planes of symmetry, or in the case of a single plane, that lies on one side. A plane of symmetry then becomes a boundary of the flow field, and its boundary condition is that the normal gradient of ln q is zero. For a rectangular grid of fluid lines on the upstream boundary, there are two convenient planes of symmetry, one of constant ψ, the other of constant η. For the polar grid arrangement, the included angle $\Delta\theta'$ (fig. 12) between two planes of symmetry can have any value that divides evenly into 360^o. In these cases of multiplane symmetry, the line of intersection between planes of symmetry is the x-axis in x,y,z-space, and, only if the flow field does not include this axis, can the duct turn.

For branched ducts, the flow field in φ,ψ,η-space can be cut by any specified line, of constant shape on ψ,η-planes, moving directly upstream in the negative φ-direction from the downstream boundary. Because the ψ and η values on the two surfaces of the cut are constant in the direction of φ, these surfaces are composed of streamlines. This cut is extended upstream to the value, or values, of φ along which the flow branches. The cut line is defined by

$$\psi_C = \psi_C(p_C) \tag{31a}$$

$$\eta_C = \eta_C(p_C) \tag{31b}$$

where p_C is path length along the cut line on ψ,η-planes in φ,ψ,η-space. Thus the velocity distributions on each of the two surfaces of the cut are prescribed separately by

$$\ln q_C = f(\varphi, p_C) \tag{31c}$$

In the region where the flow branches, a stagnation condition (q.v.) can exist, in which case, the prescribed velocity is zero. In the absence of stagnation, the prescribed velocities remain finite, and the boundary surface at the branch junction is cusped in x,y,z-space. Any number of branches for the same duct can be treated by the method just described. For any branched duct, the specified velocity distribution should be such that, in x,y,z-space, the branch turns away from, and not into, the duct or other branches. This condition is achieved by specifying higher velocities on the branch wall opposite the duct or other branches.

For ducts with centerbodies, the polar arrangement of fluid lines on the upstream boundary in x,y,z-space is required, as discussed previously. In this case, the origin, with ψ equal to 0.0 and with η having its full range of values (0.0 to 1.0), becomes a boundary surface in φ,ψ,η-space. This surface is the stagnation (or cusp) streamline upstream from the centerbody and becomes the surface of the centerbody itself downstream from the stagnation point or cusped region. Upstream from the centerbody, the boundary condition is constant ln q (value not specified, but related by the governing differential equation to the values of ln q at all adjacent grid points) for all values of η having the same value of φ. Downstream from the stagnation point, or from the cusp, the boundary condition is the specified distribution of ln q as a function of φ and η on the surface of the centerbody.

Turning angle. - The turning angle of a three-dimensional duct is given by the change in flow direction between the upstream and downstream boundaries. These flow directions are given by the direction cosines: $\cos \alpha_{1U}$, $\cos \beta_{1U}$, and $\cos \gamma_{1U}$ at the upstream boundary ($\varphi = 0.0$) and $\cos \alpha_{1D}$, $\cos \beta_{1D}$, and $\cos \gamma_{1D}$ at the downstream boundary ($\varphi = \varphi_D$). Although, for the design of two-dimensional ducts, analytical methods have been developed (ref. 1) for predicting the turning angle as a function of the prescribed velocity distribution, no attempt to do this for three-dimensional ducts is made in this report.

External Flow Fields

External flow fields are flow fields that surround bodies in x,y-z-space. The bodies can be solid or ducted. The three-dimensionality of these flow fields implies that the bodies are unsymmetrical, although the bodies can have planar symmetry.

Upstream boundary. - For external flow fields, the upstream boundary in x, y, z-space can be, for convenience, similar to that for those internal flow fields (q.v.) where a polar arrangement of fluid lines is used. However, for external flow fields, in the absence of planar symmetry, the shape of the upstream boundary in x, y, z-space can always be circular with $\Delta\theta'_U$ (fig. 12) and $r_{U,\min}$ equal to 360° and 0.0, respectively.

From equation (30c), with

$$\left.\begin{aligned} y_U &= r_{U,\max} \cos \theta'_U \\ z_U &= r_{U,\max} \sin \theta'_U \end{aligned}\right\} \tag{32a}$$

the nondimensional area A_U of the upstream boundary becomes

$$A_U = 1.0 = \frac{1}{2} \oint r^2_{U,\max}\, d\theta'_U \tag{32b}$$

from which

$$r_{U,\max} = \sqrt{\frac{1}{\pi}} \tag{32c}$$

If, by definition,

$$\eta = \frac{\theta'_U}{2\pi} \tag{32d}$$

so that the full range of η values goes from 0.0 to 1.0 as θ'_U goes from 0.0 to 2π, then, from equations (30f) and the continuity equation (9d),

$$\rho_U q_U \sin \theta_U = \frac{1}{r_U}\left(\frac{d\psi}{dr}\right)_U \left(\frac{d\eta}{d\theta'}\right)_U$$

or, because $\rho_U = 1.0$, $q_U = 1.0$, and θ_U is 90°,

$$d\psi = 2\pi r_U\, dr_U$$

from which,

$$\int_0^{\psi} d\psi = 2\pi \int_0^{r_U} r_U \, dr_U$$

or

$$\psi = \pi r_U^2 \tag{32e}$$

From equation (32e), with r_U given by equation (32c),

$$\psi_{max} = 1.0 \tag{32f}$$

so that the full range of ψ values also goes from 0.0 to 1.0, as r_U goes from 0.0 to $1/\sqrt{\pi}$.

For the given arrangement of fluid lines, the shape of the upstream boundary with a grid of ψ and η lines is that shown in figure 14, where the scale of y_U and z_U is such that the upstream area A_U is 1.0. In this figure, the stagnation (or cusp) streamline is located at the origin, where ψ is 0.0 and η has its full range of values from 0.0 to 1.0. This singularity in x,y,z-space disappears in φ,ψ,η-space, where the design problem is solved, and where the η values are finitely spaced along the boundary for ψ equal to zero. Boundary conditions along this stagnation streamline can be treated in a similar fashion to that for the stagnation streamline upstream from the centerbody in an internal flow field (q.v.). (Note that the fluid lines of constant η in figure 14 need not be equally spaced.) Downstream from the stagnation point or cusp region on the body, the value of ψ is everywhere 0.0 on the surface of the body, which surface is then covered by a network of η and φ lines. In this circular grid arrangement, unlike that for internal flow (fig. 12), the fluid lines of constant ψ are spaced closer together near the origin, as shown in figure 14. This closer spacing is used because the fluid in these stream laminae experiences greater deformations, and, therefore, requires closer attention, in passing around the body. (It is for this reason also that the fluid lines of constant η might be more closely spaced relative to one side of the body.) For external flow fields with this circular grid, it is noted that, for constant values of ψ, the spacing of interior grid points from the boundary surface is conveniently constant. Although the nondimensional radius $r_{U,max}$ of the grid is constant at $\sqrt{1/\pi}$, the dimensional value must be sufficiently large, relative to the size of the body, that the nondimensional velocity q along the surface of the cylinder in x,y,z-space is essentially constant and equal to q_U, that is, 1.0.

Grid configuration. - The boundary of the grid configuration in x,y,z-space is a right circular cylinder, as shown in figure 15, with a polar grid at the upstream boundary, as shown in figure 14. The configuration of the downstream boundary varies with

such conditions as closure (q.v.) and planar symmetry normal to the direction of undisturbed flow. The body itself is located in a small region close to, and including, the axis of the cylinder. The grid surfaces of constant φ, ψ, and η are warped (not shown) in the disturbed region of flow around the body. In this disturbed region, φ surfaces should be more closely spaced (as shown) for greater detail, as is the spacing of ψ surfaces in figure 14.

The boundary of the grid configuration in φ,ψ,η-space, which grid corresponds point for point with that in x, y, z-space, is a rectangular parallelepiped, as shown in figure 15. In this grid, unlike that in x, y, z-space, the grid points themselves occupy the corners of small rectangular parallelepipeds. This arrangement results in convenient finite-difference stars (q.v.) for the solution of the governing differential equation in φ,ψ,η-space.

Specified velocity distribution on body. - The specified velocity distributions on the upstream and downstream boundaries are uniform, unless the downstream boundary is a plane of symmetry (q.v.), in which case, the velocity is not specified on the plane of symmetry, and, instead, the boundary condition becomes $\partial \ln q/\partial\varphi = 0.0$. For those cases where the velocity is uniform, the nondimensional velocity, both upstream (q_U) and downstream (q_D), is 1.0. The dimensional value of this velocity must not be supersonic.

Provided the nondimensional radius of the essentially cylindrical boundary (fig. 15) in x, y, z-space, which radius is approximately equal to $r_{U,max}$ (equals $\sqrt{1/\pi}$), is sufficiently large relative to the size of the body, the velocity on this surface of constant ψ equal to 1.0 (fig. 14) is uniform and equal to 1.0. If $\Delta\theta'$ (fig. 12) is 360^o, that is, there is no planar symmetry parallel to the direction of flow, which is discussed later, then the velocity (not specified) is the same at corresponding φ,ψ-points on the two surfaces of constant η equal to 0.0 and 1.0.

The remaining boundary is the η,φ-surface of constant ψ equal to zero, which surface is the stagnation (or cusp) streamline upstream from the body, and becomes the body surface itself downstream from the stagnation point or cusped region. Upstream from the body, the boundary condition is that ln q (value not specified, but related by the governing differential equation to the values of ln q at all adjacent grid points) is constant for all values of η having the same value of φ. Downstream from the stagnation point or cusp, the boundary condition is the specified distribution of ln q as a function of φ and η on the body surface. And downstream from the body, the boundary condition is that ln q (value not specified, but see previous discussion for upstream stagnation streamline) is again constant for all values of η having the same value of φ. The shape of this boundary downstream from the body in x, y, z-space depends on the specified velocity distribution on the body surface. The downstream boundary should degen-

erate into the downstream stagnation streamline, but whether or not it does involves the problem of closure, which is considered briefly later in this report.

For planar symmetry (q.v.) parallel to the direction of undisturbed flow, that is, parallel to $\bar{q}_U$, only a sector of the cylinder bounded by two planes of constant θ' in x, y, z-space need be designed. These planes of symmetry then become two boundaries of the flow field, and their boundary condition is that the gradient of ln q with respect to η, that is, normal to the planes, is zero. The included angle $\Delta\theta'$ (fig. 12) between the planes of symmetry can have any value that divides equally into 360°; in particular, for $\Delta\theta'$ equal to 180°, the flow field is divided equally, with each half being a mirror image of the other.

A ducted body results if the flow field in φ, ψ, η-space (fig. 15) is cut along any plane surface of constant ψ_C greater than zero. This cut starts at the downstream boundary and extends upstream in the negative φ-direction to the value, or values, of φ corresponding to the upstream stagnation or cusped region of the body. Separate velocity distributions on each of the two surfaces of the cut are prescribed by

$$\ln q_C = f(\eta_C, \varphi_C) \tag{33}$$

As a result of this cut and of the separate velocity distributions, the surface of the ducted body in x, y, z-space has the constant value of ψ_C and is covered by a network of η and φ lines. As is the case for unducted bodies, closure (q.v.) depends on the velocity distribution prescribed on the body surface. Note that a centerbody exists within the duct if a velocity distribution is specified on the centerbody surface ($\psi = 0.0$), as described in the section Specified velocity distribution on boundary, under Internal Flow Fields. Otherwise the boundary condition for ψ equal to zero is that ln q (value not specified, but see previous discussions of boundary conditions for stagnation streamlines) is constant for all values of η having the same value of φ.

Closure. - The ψ surfaces equal to 0.0 or ψ_C define the body shape in x, y, z-space. These surfaces should, therefore, close at the downstream end of the body in x, y, z-space. Depending on the specified velocity distribution on the body itself, these ψ surfaces may close, or they may remain as finite-size (positive or negative) tails of the body, extending downstream to infinity. This closure condition for the body is not treated in this report. However, for flow fields that are symmetrical about a plane normal to the direction of undisturbed flow, which plane is halfway along the length of the body, closure is ensured by the symmetry. Also, if the tail is of modest cross section relative to the body size, it can be chopped off with no significant effect on the prescribed velocity distribution.

Numerical Procedure

The following list is a brief outline of the numerical procedure for the design of three-dimensional flow fields. For details on special situations, refer to previous sections in this report.

(1) For internal flow fields, specify the shape of the upstream boundary, that is, the upstream flow area of the duct, which boundary is the y, z-plane for x equal to zero in x, y, z-space. Compute the area of the upstream boundary, and express the y, z-coordinates of this perimeter in nondimensional units, as described in this report. For external flow problems, step (1) is not required.

(2) Prescribe the desired distributions of nondimensional velocity q as functions of nondimensional path length s along streamlines (constant ψ and η) on the undefined boundary of the flow field in x, y, z-space. These distributions with respect to s are easily converted into distributions with respect to velocity potential φ by the equation

$$\varphi = \int_0^s q(s)ds$$

Thus Q, which is ln q, is a known function of φ along streamlines on the lateral boundary. The maximum value of specified velocity, when expressed dimensionally, should not exceed the local speed of sound (except perhaps slightly, and then only for a restricted part of the boundary).

(3) Assume initial values for Q at all interior grid points of the finite-difference grid.

(4) Compute the coefficients C from equations (28f), where, for the initial finite-difference solution of the governing equation, $dn/d\psi$, $dm/d\eta$, and θ can be assigned values of 1.0, 1.0, and 90°, respectively, for a rectangular arrangement of the fluid lines on the upstream boundary. (Also, for the initial finite-difference solution, with a rectangular arrangement of the upstream fluid lines, the total curvatures K_ψ and K_η are assumed to be zero.) For a polar arrangement of the upstream fluid lines, special care is required as the radius r approaches zero.

(5) At every internal grid point, solve the finite-difference form (eq. (28e)) of the governing differential equation (17h) by using standard finite-difference procedures. Equation (28e) is solved when the highest absolute value of residual error $\mathcal{R}$ in the flow field is less than a small specified amount.

(6) At each interior grid point of the finite-difference grid, compute the direction cosines from equations (21c), (21d), (21e), (22c), (22d), (22e), (23c), (23d), and (23e).

(7) Compute the total curvatures K_η and K_ψ from equations (17f) and (17g), respectively, or from equations (C5) and (C6), respectively.

(8) Compute the angles θ from equation (8c).

(9) Determine the densities ρ from the velocities q.

(10) Determine the physical shape of the flow field in x, y, z-space by computing the x, y, z-coordinates for every point in the finite-difference grid by using equations (26a), (26d), and/or (26g) for x, equations (26b), (26e), and/or (26h) for y, and equations (26c), (26f), and/or (26i) for z.

(11) Compute the parameters A and B from equations (24) and (25), respectively. Although in theory the values of A and B are determined by equations (24) and (25), respectively, in practice, the values may be better determined, during the iteration process, by equation (10d) and the ratio of equations (24) and (25) or by equation (10d) and the difference of equations (16c) and (16d), which difference gives

$$\frac{\partial\left(\frac{A}{B}\right)}{\partial\varphi} = \frac{A}{B}\left(B\bar{e}_2 \cdot \frac{\partial\bar{e}_1}{\partial\psi} - A\bar{e}_3 \cdot \frac{\partial\bar{e}_1}{\partial\eta}\right)$$

(12) Repeat steps (4) to (11) until the value of velocity at each interior grid point has converged within a specified limit or until the maximum absolute value of the residual $\mathfrak{R}$ for a new set of coefficients C from step (4) is less than a small specified amount.

CONCLUDING REMARKS

The general design method developed in this report is for steady, three-dimensional, potential, incompressible or subsonic-compressible flow. In this design method, the flow field, including the shape of its boundary, is determined for arbitrarily specified, continuous distributions of velocity as a function of arc length along the boundary streamlines. The method applies to the design of both internal and external flow fields, including, in both cases, fields with planar symmetry. These designs result from the finite-difference solution of a governing differential equation for the distribution of velocity in transformed space, the coordinates of which are the velocity potential and two steam functions. The analytic problems associated with stagnation points, closure of bodies in external flow fields, and prediction of turning angles in three-dimensional ducts are discussed, but not treated in detail.

This three-dimensional design method applies to simple ducts, branched ducts, annular ducts, ducts with centerbodies, including the nose and/or tail region, and ducted or nonducted bodies in infinite, uniform flow fields. Solutions determine a curvilinear coordinate system in physical space for boundaries with prescribed and, therefore, basically good velocity distributions, which coordinate system, if desired, can then be used for subsequent, three-dimensional, viscous flow analyses.

APPENDIX A

ORTHOGONALITY OF STREAM SURFACES AND POTENTIAL SURFACES

Two families of surfaces are orthogonal, if the dot product of the gradients of their generating functions is zero. Thus, for potential surfaces of constant φ and stream surfaces of constant ψ,

$$\nabla\varphi \cdot \nabla\psi = \left(\bar{i}\frac{\partial\varphi}{\partial x} + \bar{j}\frac{\partial\varphi}{\partial y} + \bar{k}\frac{\partial\varphi}{\partial z}\right) \cdot \left(\bar{i}\frac{\partial\psi}{\partial x} + \bar{j}\frac{\partial\psi}{\partial y} + \bar{k}\frac{\partial\psi}{\partial z}\right)$$

$$= \frac{\partial\varphi}{\partial x}\frac{\partial\psi}{\partial x} + \frac{\partial\varphi}{\partial y}\frac{\partial\psi}{\partial y} + \frac{\partial\varphi}{\partial z}\frac{\partial\psi}{\partial z}$$

or, from equations (5d) and (6c),

$$\rho\,\nabla\varphi \cdot \nabla\psi = \left(\frac{\partial\psi}{\partial y}\frac{\partial\eta}{\partial z} - \frac{\partial\psi}{\partial z}\frac{\partial\eta}{\partial y}\right)\frac{\partial\psi}{\partial x} + \left(\frac{\partial\psi}{\partial z}\frac{\partial\eta}{\partial x} - \frac{\partial\psi}{\partial x}\frac{\partial\eta}{\partial z}\right)\frac{\partial\psi}{\partial y} + \left(\frac{\partial\psi}{\partial x}\frac{\partial\eta}{\partial y} - \frac{\partial\psi}{\partial y}\frac{\partial\eta}{\partial x}\right)\frac{\partial\psi}{\partial z}$$

$$= 0$$

so that stream surfaces of constant ψ and potential surfaces of constant φ are orthogonal.

Likewise, for stream surfaces of constant η and potential surfaces of constant φ,

$$\nabla\eta \cdot \nabla\varphi = \left(\bar{i}\frac{\partial\eta}{\partial x} + \bar{j}\frac{\partial\eta}{\partial y} + \bar{k}\frac{\partial\eta}{\partial z}\right) \cdot \left(\bar{i}\frac{\partial\varphi}{\partial x} + \bar{j}\frac{\partial\varphi}{\partial y} + \bar{k}\frac{\partial\varphi}{\partial z}\right)$$

$$= \frac{\partial\eta}{\partial x}\frac{\partial\varphi}{\partial x} + \frac{\partial\eta}{\partial y}\frac{\partial\varphi}{\partial y} + \frac{\partial\eta}{\partial z}\frac{\partial\varphi}{\partial z}$$

or, again from equations (5d) and (6c),

$$\rho\,\nabla\eta \cdot \nabla\varphi = \frac{\partial\eta}{\partial x}\left(\frac{\partial\psi}{\partial y}\frac{\partial\eta}{\partial z} - \frac{\partial\psi}{\partial z}\frac{\partial\eta}{\partial y}\right) + \frac{\partial\eta}{\partial y}\left(\frac{\partial\psi}{\partial z}\frac{\partial\eta}{\partial x} - \frac{\partial\psi}{\partial x}\frac{\partial\eta}{\partial z}\right) + \frac{\partial\eta}{\partial z}\left(\frac{\partial\psi}{\partial x}\frac{\partial\eta}{\partial y} - \frac{\partial\psi}{\partial y}\frac{\partial\eta}{\partial x}\right)$$

$$= 0$$

so that stream surfaces of constant η and potential surfaces of constant φ are orthogonal.

For the two families of stream surfaces,

$$\nabla\psi \cdot \nabla\eta = \frac{\partial\psi}{\partial x}\frac{\partial\eta}{\partial x} + \frac{\partial\psi}{\partial y}\frac{\partial\eta}{\partial y} + \frac{\partial\psi}{\partial z}\frac{\partial\eta}{\partial z}$$

which, in general, is not zero, so that the stream surfaces of constant ψ and the stream surfaces of constant η are not orthogonal. In fact, from equations (10d), (10f), and (10h),

$$\nabla\psi \cdot \nabla\eta = -\frac{\rho q}{\tan\theta} \tag{A1}$$

so that stream surfaces of constant ψ are orthogonal to stream surfaces of constant η only when θ is 90° (a truism).

However, because both families of stream surfaces are normal to the potential surfaces of constant φ, the angle θ (fig. 3) with which the stream surfaces intersect is measured on the potential surface and is given by

$$\cos\theta(\varphi,\psi,\eta) = \frac{F}{\sqrt{EG}} \tag{A2}$$

where

$$\left.\begin{aligned} E &= \left(\frac{\partial x}{\partial\psi}\right)^2 + \left(\frac{\partial y}{\partial\psi}\right)^2 + \left(\frac{\partial z}{\partial\psi}\right)^2 \\ F &= \frac{\partial x}{\partial\psi}\frac{\partial x}{\partial\eta} + \frac{\partial y}{\partial\psi}\frac{\partial y}{\partial\eta} + \frac{\partial z}{\partial\psi}\frac{\partial z}{\partial\eta} \\ G &= \left(\frac{\partial x}{\partial\eta}\right)^2 + \left(\frac{\partial y}{\partial\eta}\right)^2 + \left(\frac{\partial z}{\partial\eta}\right)^2 \end{aligned}\right\} \tag{A3}$$

The angle $\theta(\varphi,\psi,\eta)$ is also given by equation (8c).

APPENDIX B

GEODESIC CURVATURES γ OF φ, ψ, AND η CURVILINEAR COORDINATE LINES ON ψ AND η STREAM SURFACES IN x, y, z-SPACE

The local geodesic curvature of a coordinate line on a stream surface measures the local deviation of that line from the shortest distance on the surface between two local points an elemental distance apart on the line. (On a plane surface, the local geodesic curvature of a line is the reciprocal of its local radius of curvature.) From page 295 of reference 6, on a surface with u, v curvilinear coordinates, a field of curves having the unit tangent vector $\bar{e}(u, v)$ has at every point the geodesic curvature

$$\gamma = \bar{n} \cdot \nabla_S \times \bar{e} = \frac{1}{H}\left[\frac{\partial}{\partial u}\left(\frac{\partial \bar{r}}{\partial v} \cdot \bar{e}\right) - \frac{\partial}{\partial v}\left(\frac{\partial \bar{r}}{\partial u} \cdot \bar{e}\right)\right] \tag{B1}$$

where $\bar{n}$ is the unit vector normal to the surface, $\bar{r}$ is the vector position on the surface, ∇_S is the vector differential operator on the surface, and

$$H = \frac{\partial \bar{r}}{\partial u} \times \frac{\partial \bar{r}}{\partial v} \cdot \bar{n} \tag{B2}$$

First, consider the η stream surface shown in sketch (b).

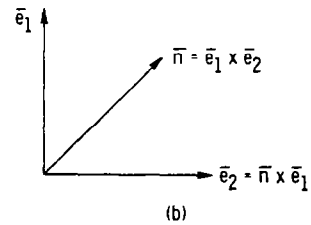

(b)

For this surface,

$$\left.\begin{aligned} \bar{n} &= \bar{e}_1 \times \bar{e}_2 \\ u &= \varphi \\ v &= \psi \end{aligned}\right\} \tag{B3}$$

From equations (10i),

$$\left.\begin{aligned} \frac{\partial \bar{r}}{\partial u} &= \frac{\partial \bar{r}}{\partial \varphi} = \frac{\partial s}{\partial \varphi}\,\bar{e}_1 = \frac{1}{q}\,\bar{e}_1 \\ \frac{\partial \bar{r}}{\partial v} &= \frac{\partial \bar{r}}{\partial \psi} = \frac{dn}{d\psi}\,\bar{e}_2 = \frac{1}{qB}\,\bar{e}_2 \end{aligned}\right\} \tag{B4}$$

$$\begin{aligned} \nabla_S &= \nabla\varphi\,\frac{\partial}{\partial \varphi} + \nabla_S\psi\,\frac{\partial}{\partial \psi} \\ &= \left(\frac{d\varphi}{ds}\,\bar{e}_1\right)\frac{\partial}{\partial \varphi} + \left(\frac{d\psi}{dn}\,\bar{e}_2\right)\frac{\partial}{\partial \psi} \\ &= q\bar{e}_1\,\frac{\partial}{\partial \varphi} + qB\bar{e}_2\,\frac{\partial}{\partial \psi} \end{aligned} \tag{B5}$$

and, from equations (B2), (B3), and (B4),

$$H = \left(\frac{1}{q}\,\bar{e}_1\right) \times \left(\frac{1}{qB}\,\bar{e}_2\right) \cdot (\bar{e}_1 \times \bar{e}_2) = \frac{1}{q^2 B} \tag{B6}$$

Thus, for the φ-coordinate curve on the η stream surface, with $\bar{e}$ equal to $\bar{e}_1$, equations (B1), (B3), (B4), (B5), and (B6) give

$$\gamma_1 = (\bar{e}_1 \times \bar{e}_2) \cdot \left(q\bar{e}_1 \times \frac{\partial \bar{e}_1}{\partial \varphi} + qB\bar{e}_2 \times \frac{\partial \bar{e}_1}{\partial \psi}\right) = q^2 B\left[\frac{\partial}{\partial \varphi}\left(\frac{1}{qB}\,\bar{e}_2 \cdot \bar{e}_1\right) - \frac{\partial}{\partial \psi}\left(\frac{1}{q}\,\bar{e}_1 \cdot \bar{e}_1\right)\right]$$

which reduces to

$$\frac{\gamma_1}{q} = \bar{e}_2 \cdot \frac{\partial \bar{e}_1}{\partial \varphi} = B\,\frac{\partial \ln q}{\partial \psi} \tag{B7}$$

so that

$$\bar{e}_2 \cdot \frac{\partial \bar{e}_1}{\partial \varphi} - B\,\frac{\partial \ln q}{\partial \psi} = 0 \tag{13e}$$

Equation (13e) is the irrotationality condition on the η stream surface.

Likewise, for the ψ-coordinate curve on the η-surface, with $\bar{e}$ equal to $\bar{e}_2$, equations (B1), (B3), (B4), (B5), and (B6) give

$$-\frac{\gamma_2}{q} = B\bar{e}_1 \cdot \frac{\partial \bar{e}_2}{\partial \psi} = \frac{\partial \ln q}{\partial \varphi} + \frac{\partial \ln B}{\partial \varphi}$$

However,

$$\bar{e}_1 \cdot \bar{e}_2 = 0$$

so that

$$\bar{e}_1 \cdot \frac{\partial \bar{e}_2}{\partial \psi} = -\bar{e}_2 \cdot \frac{\partial \bar{e}_1}{\partial \psi}$$

and, thus,

$$\frac{\gamma_2}{q} = B\bar{e}_2 \cdot \frac{\partial \bar{e}_1}{\partial \psi} = -\frac{\partial \ln q}{\partial \varphi} - \frac{\partial \ln B}{\partial \varphi} \tag{B8}$$

or

$$B\bar{e}_2 \cdot \frac{\partial \bar{e}_1}{\partial \psi} = -\frac{\partial \ln q}{\partial \varphi} - \frac{\partial \ln B}{\partial \varphi} \tag{16c}$$

Equation (16c) is the continuity condition for flow in η stream laminae.

Next, consider the ψ stream surface shown in sketch (c).

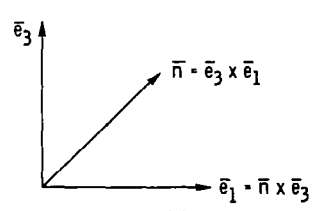

(c)

For this surface,

$$\left.\begin{aligned} \bar{n} &= \bar{e}_3 \times \bar{e}_1 \\ u &= \eta \\ v &= \varphi \end{aligned}\right\} \tag{B9}$$

From equations (10i),

$$\left.\begin{aligned} \frac{\partial \bar{r}}{\partial u} &= \frac{\partial \bar{r}}{\partial \eta} = \frac{dm}{d\eta}\,\bar{e}_3 = \frac{1}{qA}\,\bar{e}_3 \\ \frac{\partial \bar{r}}{\partial v} &= \frac{\partial \bar{r}}{\partial \varphi} = \frac{ds}{d\varphi}\,\bar{e}_1 = \frac{1}{q}\,\bar{e}_1 \end{aligned}\right\} \tag{B10}$$

$$\nabla_S = \nabla_S \eta \frac{\partial}{\partial \eta} + \nabla \varphi \frac{\partial}{\partial \varphi}$$

$$= \left(\frac{d\eta}{dm}\,\bar{e}_3\right)\frac{\partial}{\partial \eta} + \left(\frac{d\varphi}{ds}\,\bar{e}_1\right)\frac{\partial}{\partial \varphi}$$

$$= qA\bar{e}_3 \frac{\partial}{\partial \eta} + q\bar{e}_1 \frac{\partial}{\partial \varphi} \tag{B11}$$

and, from equations (B2), (B9), and (B10),

$$H = \frac{1}{q^2 A} \tag{B12}$$

Thus, for the η-coordinate curve on the ψ stream surface, with $\bar{e}$ equal to $\bar{e}_3$, equations (B1), (B9), (B10), (B11), and (B12) give

$$-\frac{\gamma_3}{q} = A\bar{e}_3 \cdot \frac{\partial \bar{e}_1}{\partial \eta} = -\frac{\partial \ln q}{\partial \varphi} - \frac{\partial \ln A}{\partial \varphi} \tag{B13}$$

or

$$A\bar{e}_3 \cdot \frac{\partial \bar{e}_1}{\partial \eta} = -\frac{\partial \ln q}{\partial \varphi} - \frac{\partial \ln A}{\partial \varphi} \tag{16d}$$

Equation (16d) is the continuity condition for flow in ψ stream laminae.

Likewise, for the φ-coordinate curve on the ψ-surface, with $\bar{e}$ equal to $\bar{e}_1$, equations (B1), (B9), (B10), (B11), and (B12) give

$$-\frac{\gamma_1}{q} = \bar{e}_3 \cdot \frac{\partial \bar{e}_1}{\partial \varphi} = A \frac{\partial \ln q}{\partial \eta} \tag{B14}$$

or

$$A \frac{\partial \ln q}{\partial \eta} - \bar{e}_3 \cdot \frac{\partial \bar{e}_1}{\partial \varphi} = 0 \tag{13f}$$

Equation (13f) is the irrotationality condition on the ψ stream surface.

APPENDIX C

TOTAL CURVATURES K OF ψ AND η STREAM SURFACES IN x, y, z-SPACE

From page 306 of reference 6, the local total curvature K_η of the η stream surface is given by

$$-K_\eta = \frac{1}{H}\left[\frac{\partial}{\partial\varphi}\left(\frac{\partial\bar{r}}{\partial\psi}\cdot\bar{R}\right) - \frac{\partial}{\partial\psi}\left(\frac{\partial\bar{r}}{\partial\varphi}\cdot\bar{R}\right)\right] \tag{C1}$$

where

$$\bar{R} = \gamma_1\bar{e}_1 + \gamma_2\bar{e}_2 \tag{C2}$$

and H, $\partial\bar{r}/\partial\psi$, $\partial\bar{r}/\partial\varphi$, γ_1, and γ_2 are given by equations (B6), (B4), (B4), (B7), and (B8), respectively. Thus

$$-K_\eta = q^2 B\left[\frac{\partial}{\partial\varphi}\left(\bar{e}_2\cdot\frac{\partial\bar{e}_1}{\partial\psi}\right) - \frac{\partial}{\partial\psi}\left(\bar{e}_2\cdot\frac{\partial\bar{e}_1}{\partial\varphi}\right)\right]$$

which reduces to

$$-\frac{K_\eta}{q^2} = B\left(\frac{\partial\bar{e}_2}{\partial\varphi}\cdot\frac{\partial\bar{e}_1}{\partial\psi} - \frac{\partial\bar{e}_2}{\partial\psi}\cdot\frac{\partial\bar{e}_1}{\partial\varphi}\right) \tag{17f}$$

Equation (17f) gives the value of K_η/q^2 in the governing differential equation (17h).

Likewise the total curvature K_ψ of the ψ stream surface is given by

$$-K_\psi = \frac{1}{H}\left[\frac{\partial}{\partial\eta}\left(\frac{\partial\bar{r}}{\partial\varphi}\cdot\bar{R}\right) - \frac{\partial}{\partial\varphi}\left(\frac{\partial\bar{r}}{\partial\eta}\cdot\bar{R}\right)\right] \tag{C3}$$

where

$$\bar{R} = \gamma_3\bar{e}_3 + \gamma_1\bar{e}_1 \tag{C4}$$

and H, $\partial\bar{r}/\partial\varphi$, $\partial\bar{r}/\partial\eta$, γ_3, and γ_1 are given by equations (B12), (B10), (B10), (B13), and (B14), respectively. Thus

$$-K_\psi = q^2 A\left[\frac{\partial}{\partial\eta}\left(-\bar{e}_3 \cdot \frac{\partial \bar{e}_1}{\partial\varphi}\right) - \frac{\partial}{\partial\varphi}\left(-\bar{e}_3 \cdot \frac{\partial \bar{e}_1}{\partial\eta}\right)\right]$$

which reduces to

$$-\frac{K_\psi}{q^2} = A\left(\frac{\partial \bar{e}_3}{\partial\varphi} \cdot \frac{\partial \bar{e}_1}{\partial\eta} - \frac{\partial \bar{e}_3}{\partial\eta} \cdot \frac{\partial \bar{e}_1}{\partial\varphi}\right) \tag{17g}$$

Equation (17g) gives the value of K_ψ/q^2 in the governing differential equation (17h).

From equations (B7), (B8), (B13), and (B14), the geodesic curvatures γ, and, therefore, the total curvatures K, can be expressed in terms of velocity rather than unit vectors. Thus, for the η stream surface, from equations (C1), (C2), (B4), (B6), (B7), and (B8),

$$-K_\eta = q^2 B\left\{\frac{\partial}{\partial\varphi}\left[\frac{1}{B}\left(-\frac{\partial \ln q}{\partial\varphi} - \frac{\partial \ln B}{\partial\varphi}\right)\right] - \frac{\partial}{\partial\psi}\left(B\,\frac{\partial \ln q}{\partial\psi}\right)\right\}$$

which expands to

$$-\frac{K_\eta}{q^2} = \frac{\partial \ln B}{\partial\varphi}\left(\frac{\partial \ln q}{\partial\varphi} + \frac{\partial \ln B}{\partial\varphi}\right) - \frac{\partial^2 \ln q}{\partial\varphi^2} - \frac{\partial^2 \ln B}{\partial\varphi^2} - B^2\left(\frac{\partial \ln B}{\partial\psi}\,\frac{\partial \ln q}{\partial\psi} + \frac{\partial^2 \ln q}{\partial\psi^2}\right) \tag{C5}$$

Likewise, for the ψ stream surface, from equations (C3), (C4), (B10), (B12), (B13), and (B14),

$$-K_\psi = q^2 A\left\{\frac{\partial}{\partial\eta}\left(-A\,\frac{\partial \ln q}{\partial\eta}\right) - \frac{\partial}{\partial\varphi}\left[\frac{1}{A}\left(\frac{\partial \ln q}{\partial\varphi} + \frac{\partial \ln A}{\partial\varphi}\right)\right]\right\}$$

which expands to

$$-\frac{K_\psi}{q^2} = \frac{\partial \ln A}{\partial\varphi}\left(\frac{\partial \ln q}{\partial\varphi} + \frac{\partial \ln A}{\partial\varphi}\right) - \frac{\partial^2 \ln q}{\partial\varphi^2} - \frac{\partial^2 \ln A}{\partial\varphi^2} - A^2\left(\frac{\partial \ln A}{\partial\eta}\,\frac{\partial \ln q}{\partial\eta} + \frac{\partial^2 \ln q}{\partial\eta^2}\right) \tag{C6}$$

If equations (C5) and (C6) are introduced into equation (17h), the governing differential equation becomes

$$-\frac{\partial^2 \ln q}{\partial \varphi^2} + \frac{\partial^2 \ln \rho}{\partial \varphi^2} + \frac{\partial^2 \ln \sin \theta}{\partial \varphi^2} - \frac{\partial^2 \ln B}{\partial \varphi^2} - \frac{\partial^2 \ln A}{\partial \varphi^2} = 0$$

from which, assuming the constants of integration are zero,

$$\rho \sin \theta = qAB$$

which is the continuity equation (10d).

APPENDIX D

ALTERNATIVE DERIVATION OF GOVERNING PARTIAL-DIFFERENTIAL EQUATION

In addition to its derivation in the main text of this report, the governing, second-order, partial-differential equation for the distribution of $\ln q$ in φ, ψ, η-space can be derived from separate considerations of the two-dimensional continuity and irrotationality conditions on the η and ψ stream surfaces, the results of which are then interrelated by the simple continuity equation (10d) for three-dimensional flow.

From the two-dimensional, continuity equations (16c) and (16d), or, from equations (B8) and (B13), which are the same,

$$-\frac{\partial \ln B}{\partial \varphi}\left(\frac{\partial \ln q}{\partial \varphi}+\frac{\partial \ln B}{\partial \varphi}\right)+B\frac{\partial \bar{e}_2}{\partial \varphi}\cdot\frac{\partial \bar{e}_1}{\partial \psi}+B\bar{e}_2\cdot\frac{\partial^2 \bar{e}_1}{\partial \varphi\,\partial \psi}=-\frac{\partial^2 \ln q}{\partial \varphi^2}-\frac{\partial^2 \ln B}{\partial \varphi^2} \tag{D1}$$

$$-\frac{\partial \ln A}{\partial \varphi}\left(\frac{\partial \ln q}{\partial \varphi}+\frac{\partial \ln A}{\partial \varphi}\right)+A\frac{\partial \bar{e}_3}{\partial \varphi}\cdot\frac{\partial \bar{e}_1}{\partial \eta}+A\bar{e}_3\cdot\frac{\partial^2 \bar{e}_1}{\partial \varphi\,\partial \eta}=-\frac{\partial^2 \ln q}{\partial \varphi^2}-\frac{\partial^2 \ln A}{\partial \varphi^2} \tag{D2}$$

Equations (D1) and (D2) are the two-dimensional, continuity equations in the η and ψ stream laminae, respectively.

From the two-dimensional, irrotationality equations (13e) and (13f), or, from equations (B7) and (B14), which are the same,

$$B\frac{\partial \bar{e}_2}{\partial \psi}\cdot\frac{\partial \bar{e}_1}{\partial \varphi}+B\bar{e}_2\cdot\frac{\partial^2 \bar{e}_1}{\partial \varphi\,\partial \psi}=B^2\left(\frac{\partial \ln B}{\partial \psi}\,\frac{\partial \ln q}{\partial \psi}+\frac{\partial^2 \ln q}{\partial \psi^2}\right) \tag{D3}$$

$$A\frac{\partial \bar{e}_3}{\partial \eta}\cdot\frac{\partial \bar{e}_1}{\partial \varphi}+A\bar{e}_3\cdot\frac{\partial^2 \bar{e}_1}{\partial \varphi\,\partial \eta}=A^2\left(\frac{\partial \ln A}{\partial \eta}\,\frac{\partial \ln q}{\partial \eta}+\frac{\partial^2 \ln q}{\partial \eta^2}\right) \tag{D4}$$

Equations (D3) and (D4) are the two-dimensional, irrotationality equations on the η and ψ stream surfaces, respectively.

Combining equations (D1) and (D3) to eliminate $\partial^2 \bar{e}_1/\partial \varphi\,\partial \psi$ and introducing the total curvature K_η from equation (17f) give

$$-\frac{\partial \ln B}{\partial \varphi}\left(\frac{\partial \ln q}{\partial \varphi}+\frac{\partial \ln B}{\partial \varphi}\right)-\frac{K_\eta}{q^2}+B^2\left(\frac{\partial \ln B}{\partial \psi}\,\frac{\partial \ln q}{\partial \psi}+\frac{\partial^2 \ln q}{\partial \psi^2}\right)=-\frac{\partial^2 \ln q}{\partial \varphi^2}-\frac{\partial^2 \ln B}{\partial \varphi^2} \qquad \text{(D5)}$$

Equation (D5) is the equation for two-dimensional flow in η stream laminae.

Combining equations (D2) and (D4) to eliminate $\partial^2 \overline{e}_1/\partial\varphi\,\partial\eta$ and introducing the total curvature K_ψ from equation (17g) give

$$-\frac{\partial \ln A}{\partial \varphi}\left(\frac{\partial \ln q}{\partial \varphi}+\frac{\partial \ln A}{\partial \varphi}\right)-\frac{K_\psi}{q^2}+A^2\left(\frac{\partial \ln A}{\partial \eta}\,\frac{\partial \ln q}{\partial \eta}+\frac{\partial^2 \ln q}{\partial \eta^2}\right)=-\frac{\partial^2 \ln q}{\partial \varphi^2}-\frac{\partial^2 \ln A}{\partial \varphi^2} \qquad \text{(D6)}$$

Equation (D6) is the equation for two-dimensional flow in ψ stream laminae.

From the simple continuity equation (10d) for three-dimensional flow,

$$-\frac{\partial^2 \ln q}{\partial \varphi^2}-\frac{\partial^2 \ln A}{\partial \varphi^2}-\frac{\partial^2 \ln B}{\partial \varphi^2}=-\frac{\partial^2 \ln \rho}{\partial \varphi^2}-\frac{\partial^2 \ln \sin \theta}{\partial \varphi^2}$$

from which, after equations (D5) and (D6) are added,

$$\frac{\partial^2 \ln q}{\partial \varphi^2}+\frac{\partial^2 \ln \rho}{\partial \varphi^2}+\frac{\partial^2 \ln \sin \theta}{\partial \varphi^2}-\frac{K_\psi}{q^2}-\frac{K_\eta}{q^2}+B^2\left(\frac{\partial \ln B}{\partial \psi}\,\frac{\partial \ln q}{\partial \psi}+\frac{\partial^2 \ln q}{\partial \psi^2}\right)$$

$$+A^2\left(\frac{\partial \ln A}{\partial \eta}\,\frac{\partial \ln q}{\partial \eta}+\frac{\partial^2 \ln q}{\partial \eta^2}\right)-\frac{\partial \ln B}{\partial \varphi}\left(\frac{\partial \ln q}{\partial \varphi}+\frac{\partial \ln B}{\partial \varphi}\right)-\frac{\partial \ln A}{\partial \varphi}\left(\frac{\partial \ln q}{\partial \varphi}+\frac{\partial \ln A}{\partial \varphi}\right)=0$$

(17h)

Equation (17h) is the governing differential equation for the distribution of $\ln q$ in φ, ψ, η-space as developed previously in the main text of this report.

REFERENCES

1. Stanitz, John D.: Design of Two-Dimensional Channels with Prescribed Velocity Distributions Along the Walls. NACA Rep. 1115, 1953. (Supersedes NACA TN 2593 and TN 2595.)

2. Yang, Tah-teh; Hudson, William G.; and Nelson, Carl D.: Design and Experimental Performance of Short Curved Wall Diffusers with Axial Symmetry Utilizing Slot Suction. NASA CR-2209, 1973.

3. Yih, Chia-Shun: Stream Functions in Three-Dimensional Flows. La Houille Blanche, vol. 12, no. 3, July-Aug. 1957, pp. 439-444.

4. Milne-Thomson, L. M.: Theoretical Hydrodynamics. The Macmillan Co., 1950.

5. Phillips, H. B.: Vector Analysis. John Wiley & Sons, Inc., 1933.

6. Brand, Louis: Vector and Tensor Analysis. John Wiley & Sons, Inc., 1947.

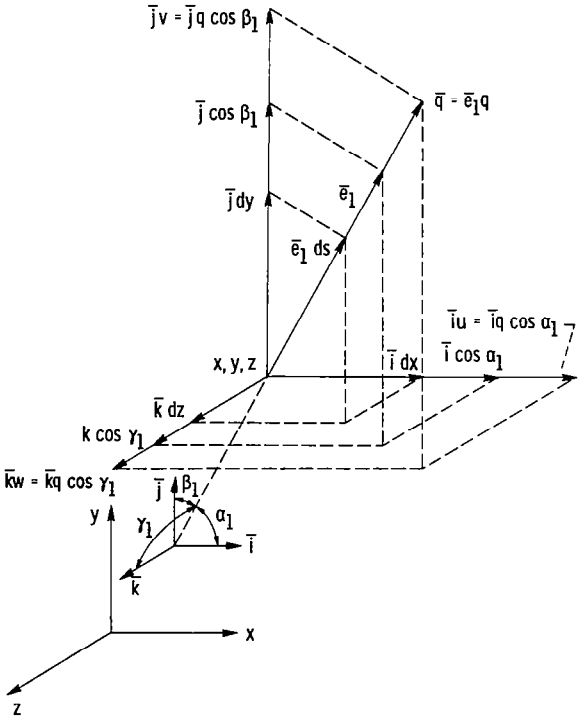

Figure 1. - Velocity vector $\bar{q}$, unit vector $\bar{e}_1$, and elemental vector distance $\bar{e}_1\,ds$ along streamline at arbitrary point of flow field in x, y, z-space together with the x, y, z-components of these vectors and the angles α_1, β_1, and γ_1 for their direction cosines.

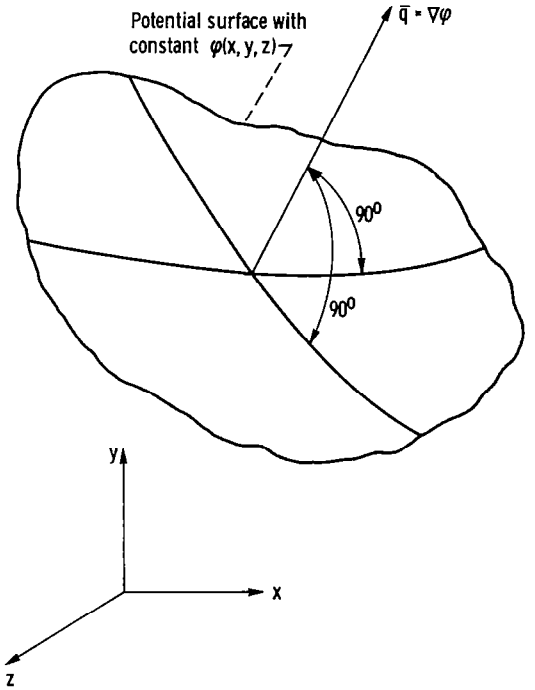

Figure 2. - Velocity vector $\bar{q}$, equal to vector gradient $\nabla\varphi$ of velocity potential and, therefore, normal to potential surface of constant φ in flow field of x, y, z-space.

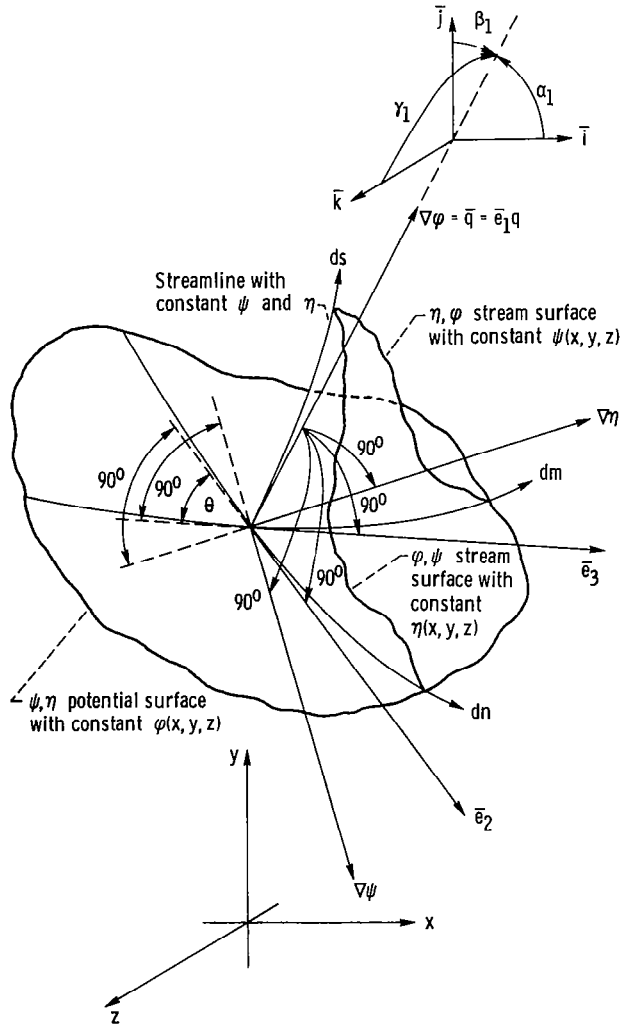

Figure 3. - Structure of flow field in x, y, z-space, showing velocity vector $\bar{q}$; ψ, η potential surface of constant φ; φ, ψ and η, φ stream surfaces of constant η and ψ, respectively; vector gradients of φ, ψ, and η; angle θ; and differential path lengths ds, dn, and dm.

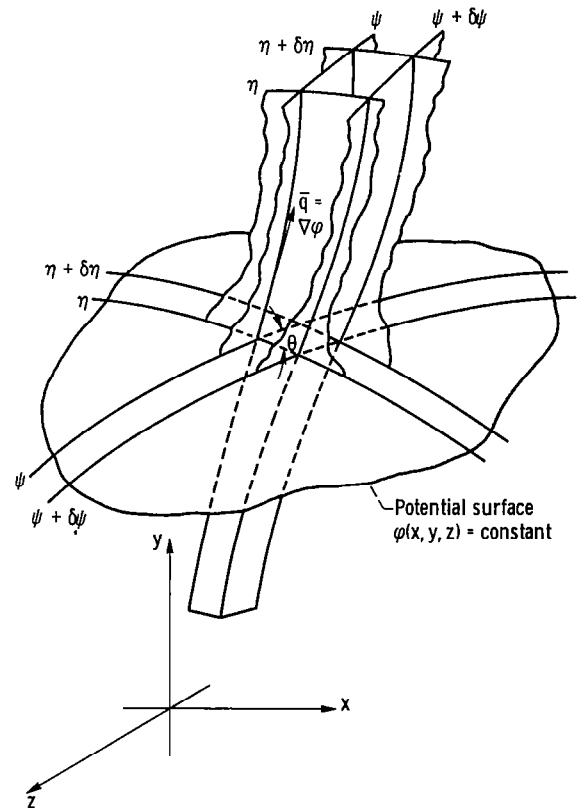

Figure 4. - Stream tube bounded by adjacent stream surfaces of constant ψ and η.

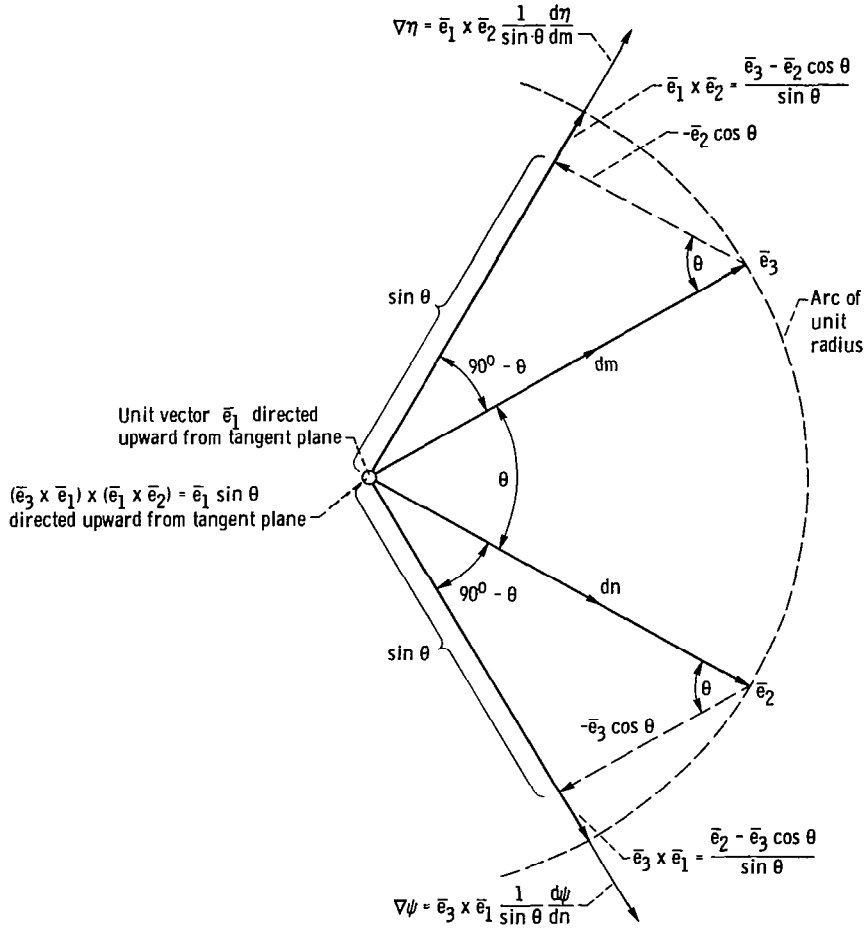

Figure 5. - Sketch of vector gradients $\nabla\psi$ and $\nabla\eta$ of stream functions on potential surface of constant φ, showing relations among these gradients, the angle θ, and various unit vectors.

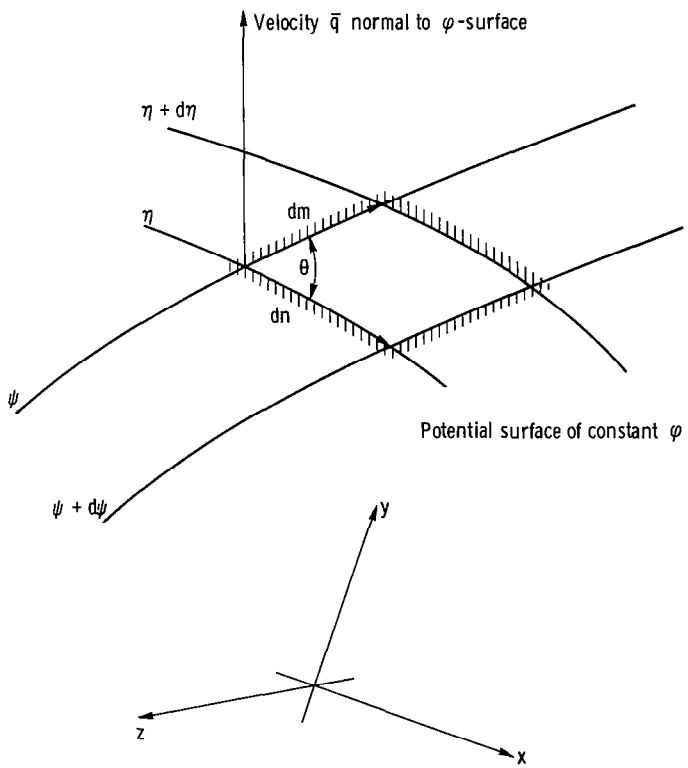

Figure 6. - Elemental flow area dn dm sin θ on potential surface of constant φ in x, y, z-space.

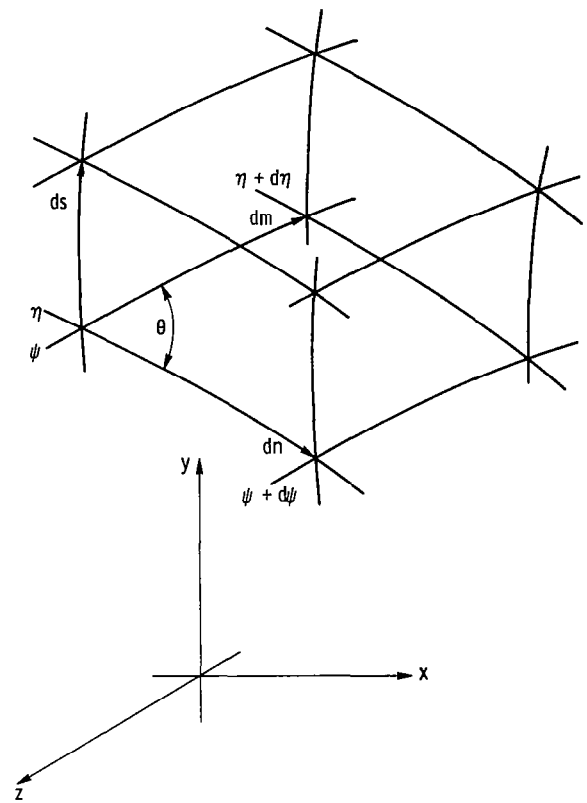

Figure 7. - Elemental volume ds dn dm sin θ bound by adjacent surfaces of constant φ, ψ, and η in x, y, z-space.

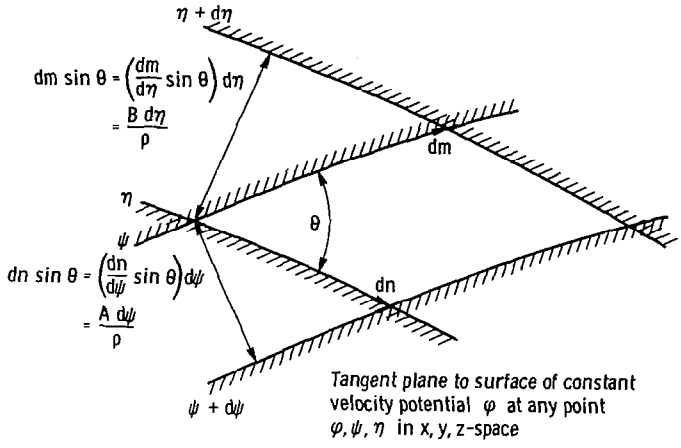

Figure 8. - Sections of three-dimensional stream laminae resulting from intersections of adjacent stream surfaces of constant ψ and η with potential surface of constant φ in this figure; velocity $\bar{q}$ is normal to these sections.

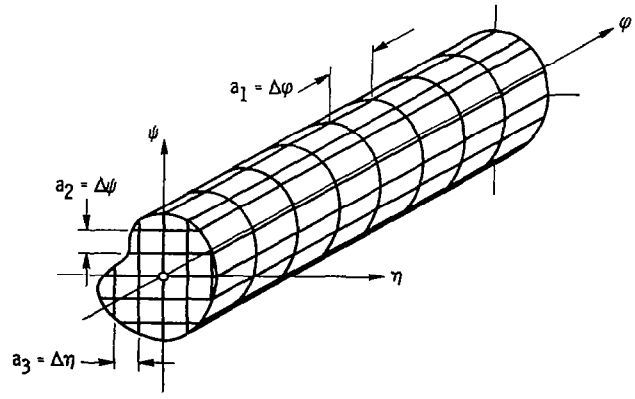

Figure 9. - Shape of flow field in transformed φ, ψ, η-space, showing spacings a_1, a_2, and a_3 between adjacent points in finite-difference grid formed by surfaces of constant φ, ψ, and η.

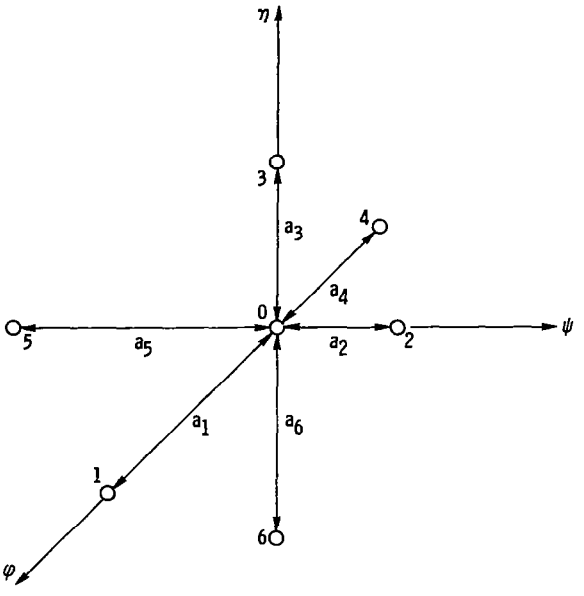

Figure 10. - Finite-difference star in transformed φ, ψ, η-space with central grid point 0 and adjacent grid points 1 to 6; variable spacing between adjacent grid points.

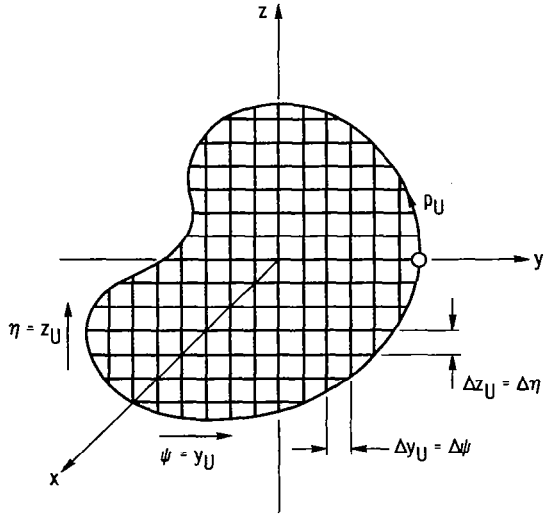

Figure 11. - Arbitrarily specified shape of upstream boundary for internal flow field in x, y, z-space. For nondimensional variables, as defined in report, ψ and η equal y_U and z_U, respectively, when θ is 90^0 on upstream boundary.

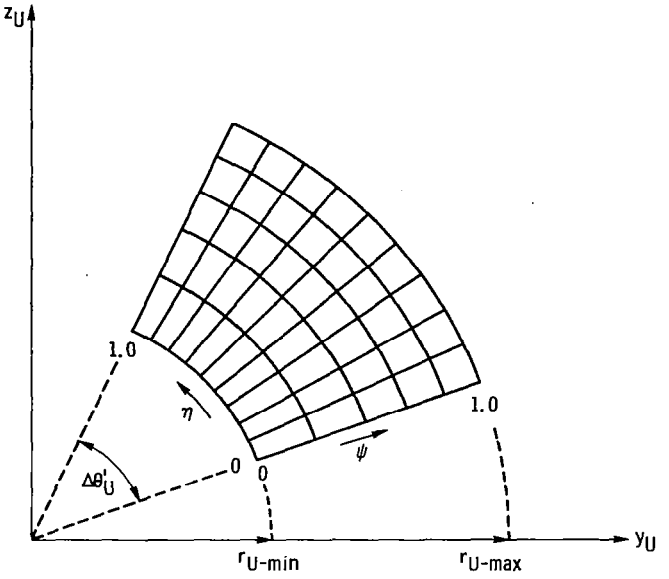

Figure 12. - Polar arrangement of fluid lines on upstream boundary for internal flow fields in x, y, z-apace; upstream flow area ($x_U = 0$, $\varphi_U = 0$), viewed by looking upstream in negative x-direction.

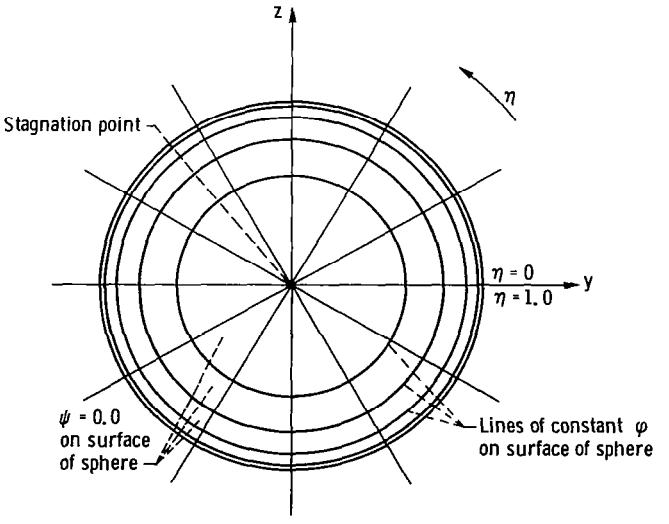

Figure 13. - Network of φ and η coordinate lines and constant (zero) value of stream function ψ on surface of sphere for incompressible, potential flow in x, y, z-space.

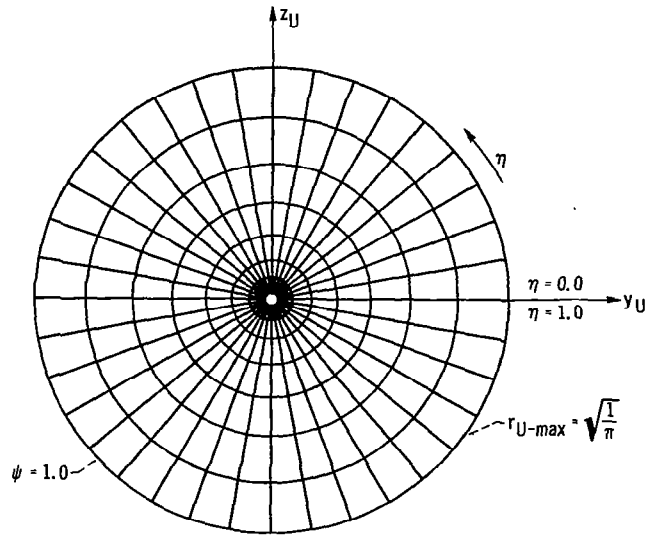

Figure 14. - Polar arrangement of fluid lines on upstream boundary for external flow fields in x, y, z-space.

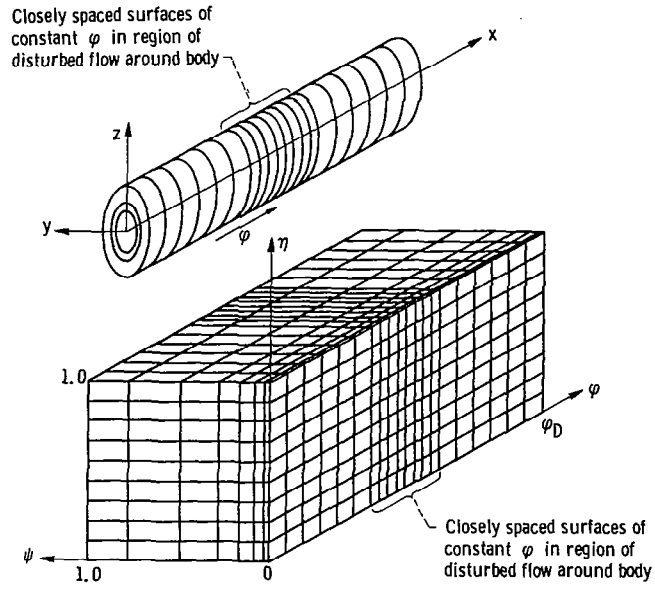

Figure 15. - Corresponding shapes of finite-difference grids in physical x, y, z-space and transformed φ, ψ, η-space for external flow fields with polar arrangement of fluid lines on upstream boundary in physical flow field.

1. Report No.	2. Government Accession No.	3. Recipient's Catalog No.
NASA CR-3288		

4. Title and Subtitle	5. Report Date
GENERAL DESIGN METHOD FOR THREE-DIMENSIONAL, POTENTIAL FLOW FIELDS I - THEORY	August 1980
	6. Performing Organization Code
7. Author(s)	8. Performing Organization Report No.
John D. Stanitz	
	10. Work Unit No.
9. Performing Organization Name and Address	
John D. Stanitz, Consulting Engineer 14475 East Carroll Boulevard University Heights, Ohio 44118	11. Contract or Grant No. NAS3-21605
	13. Type of Report and Period Covered
12. Sponsoring Agency Name and Address	Contractor Report
National Aeronautics and Space Administration Washington, D.C. 20546	14. Sponsoring Agency Code

15. Supplementary Notes

Lewis Technical Monitor: Theodore Katsanis

Final Report

16. Abstract

The general design method developed in this report is for steady, three-dimensional, potential, incompressible or subsonic-compressible flow. In this design method, the flow field, including the shape of its boundary, is determined for arbitrarily specified, continuous distributions of velocity as a function of arc length along the boundary streamlines. The method applies to the design of both internal and external flow fields, including, in both cases, fields with planar symmetry. The analytic problems associated with stagnation points, closure of bodies in external flow fields, and prediction of turning angles in three-dimensional ducts are discussed, but not treated in detail.

17. Key Words (Suggested by Author(s))		18. Distribution Statement
Design	External fluid dynamics	Unclassified - unlimited
Three-dimensional	Internal fluid dynamics	STAR Category 02
Compressible		

19. Security Classif. (of this report)	20. Security Classif. (of this page)	21. No. of Pages	22. Price*
Unclassified	Unclassified	82	A05

* For sale by the National Technical Information Service, Springfield, Virginia 22161

NASA-Langley, 1980